Cell Reports
Medicine

Article

Hybrid immunity expands the functional humoral footprint of both mRNA and vector-based SARS-CoV-2 vaccines

Graphical abstract

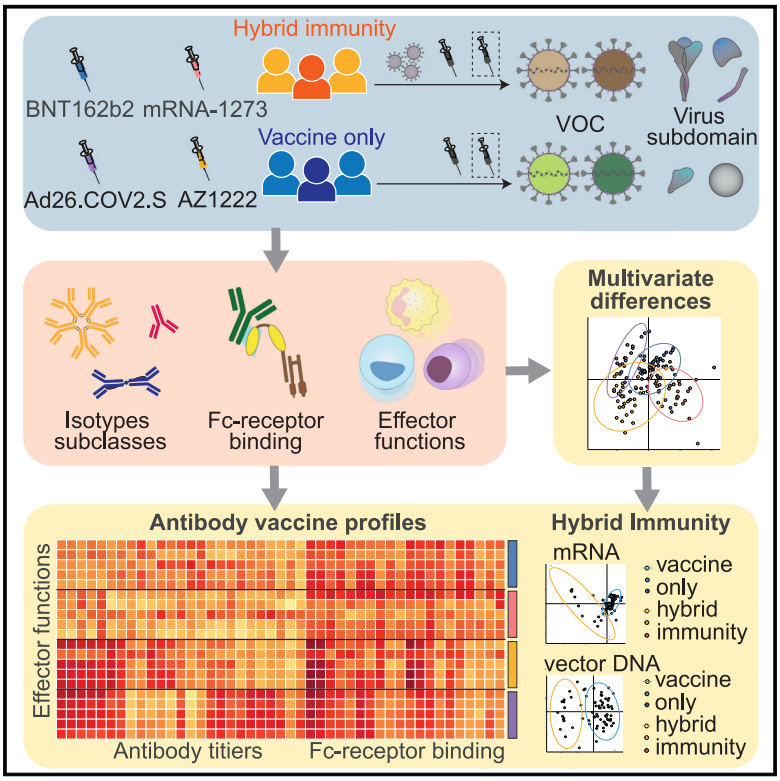

Authors

Paulina Kaplonek, Yixiang Deng, Jessica Shih-Lu Lee, ..., Douglas A. Lauffenburger, David Goldblatt, Galit Alter

Correspondence

d.goldblatt@ucl.ac.uk (D.G.), galter@mgh.harvard.edu (G.A.)

In brief

Kaplonek et al. show that mRNA- and vector-based SARS-CoV-2 vaccines display distinct immune profiles in individuals vaccinated only or infected and vaccinated. Infection prior to vaccination helps improve immunity and triggers a response to the more conserved domain of SARS-CoV-2, which might enhance the effectiveness of vaccines against new variants.

Highlights

- Each vaccine triggers a unique immune profile for vaccination-only and hybrid immunity
- Hybrid immunity shows distinct response compared with vaccination only
- Hybrid immunity improves the functional breadth of SARS-CoV-2 VOC responses
- Hybrid immunity exhibits an augmentation of S2-domain-specific functional immunity

Kaplonek et al., 2023, Cell Reports Medicine *4*, 101048
May 16, 2023
https://doi.org/10.1016/j.xcrm.2023.101048

CellPress

Cell Reports Medicine

CellPress
OPEN ACCESS

Article

Hybrid immunity expands the functional humoral footprint of both mRNA and vector-based SARS-CoV-2 vaccines

Paulina Kaplonek,[1,7] Yixiang Deng,[1,6,7] Jessica Shih-Lu Lee,[1] Heather J. Zar,[2,3] Dace Zavadska,[4] Marina Johnson,[5] Douglas A. Lauffenburger,[6] David Goldblatt,[5,*] and Galit Alter[1,8,*]

[1]Ragon Institute of Mass General, MIT, and Harvard, Cambridge, MA, USA
[2]Department of Pediatrics and Child Health, Red Cross War Memorial Children's Hospital, University of Cape Town, Cape Town, South Africa
[3]SA MRC Unit on Child and Adolescent Health, University of Cape Town, Cape Town, South Africa
[4]Children's Clinical University Hospital, Riga, Latvia
[5]Great Ormond Street Institute of Child Health Biomedical Research Centre, University College London, London, UK
[6]Department of Biological Engineering, Massachusetts Institute of Technology, Cambridge, MA, USA
[7]These authors contributed equally
[8]Lead contact
*Correspondence: d.goldblatt@ucl.ac.uk (D.G.), galter@mgh.harvard.edu (G.A.)
https://doi.org/10.1016/j.xcrm.2023.101048

SUMMARY

Despite the successes of current coronavirus disease 2019 (COVID-19) vaccines, waning immunity, the emergence of variants of concern, and breakthrough infections among vaccinees have begun to highlight opportunities to improve vaccine platforms. Real-world vaccine efficacy studies have highlighted the reduced risk of breakthrough infections and diseases among individuals infected and vaccinated, referred to as hybrid immunity. Thus, we sought to define whether hybrid immunity shapes the humoral immune response to severe acute respiratory syndrome coronavirus 2 (SARS-CoV-2) following Pfizer/BNT162b2, Moderna mRNA-1273, ChadOx1/AZD1222, and Ad26.COV2.S vaccination. Each vaccine exhibits a unique functional humoral profile in vaccination only or hybrid immunity. However, hybrid immunity shows a unique augmentation of S2-domain-specific functional immunity that was poorly induced for the vaccination only. These data highlight the importance of natural infection in breaking the immunodominance away from the evolutionarily unstable S1 domain and potentially affording enhanced cross-variant protection by targeting the more highly conserved S2 domain of SARS-CoV-2.

INTRODUCTION

The emergence of severe acute respiratory syndrome coronavirus 2 (SARS-CoV-2) in late 2019 launched an unparalleled global pandemic, causing nearly half a billion documented infections and over 6 million deaths.[1] The unpredictable trajectory of disease severity drove an urgent need for vaccine development, which proceeded at an unprecedented speed, leading to authorization and licensure of several new vaccine platforms.[2] Specifically, the Pfizer/BioNTech and Moderna mRNA vaccines were associated with greater protection against severe disease and death[3,4] than the AstraZeneca chimpanzee adenovirus (ChadOx1/AZD1222)[5] and Johnson & Johnson-Janssen adenovirus 26 (Ad26.COV2.S) vaccines.[6] Neutralizing antibodies were linked to protective immunity across all platforms during the initial phase 2b/3 trials, when the D614G strain dominated the global pandemic.[3–6] However, the emergence of several neutralization-resistant variants of concern (VOCs), in the setting of rapidly waning neutralizing antibodies caused widespread infection in the absence of a proportional increase in severe disease and death. Instead, these data suggest that alternate vaccine-induced immune responses, including T cells[7–10] and non-neutralizing antibody functions,[11,12] likely contribute to vaccine-induced attenuation of disease. However, while T cells are induced variably by these four vaccine platforms, whether non-neutralizing antibodies differ among vaccine platforms and contribute differentially to protection against severe disease and death remains unclear.

Beyond the robust correlation between neutralizing antibody titers and vaccine efficacy in early efficacy trials,[13–15] meta-analyses across vaccine trials pointed to a stronger correlation between antibody binding titers and efficacy between vaccine platforms.[16] These data pointed to the possibility that additional functions of antibodies, beyond their ability to bind and block infection, may play a critical role in the attenuation of disease. Along these lines, cytotoxic functions of antibodies were linked to survival in a large convalescent plasma therapy trial,[17] antibody Fc-effector functions are key to the therapeutic activity of several monoclonal therapeutics,[18] and the opsonophagocytic function of antibodies is a key predictor of survival of severe

natural infection.[19,20] However, whether these functions are tuned distinctly across vaccine platforms or linked to the protection afforded by specific vaccines remains unclear.

Real-world efficacy data have shown an increase vaccine effectiveness among individuals who were previously infected and then vaccinated, also referred to as hybrid immunity.[21,22] Moreover, several studies have suggested that hybrid immunity is associated with improved protection against multiple VOCs,[23–25] including Omicron,[26,27] via induction of antibodies with increased potency and breadth. Additional studies have revealed more robust spike-specific antibody production[28–30] and more vigorous T cell responses[31,32] in the setting of hybrid immunity. However, whether hybrid immunity also alters the functional character of the humoral immune response remains unclear.

Preliminary data have pointed to subtle differences in the vaccine-induced antibody profiles between the Pfizer/BioNTech BNT162b2 and Moderna mRNA-1273 mRNA vaccines.[12] However, whether these functional humoral responses differ among adenovirus viral vaccines as well, and whether they are tuned in the setting of hybrid immunity, has remained unclear. Thus, here we deeply profiled the functional humoral immune response across four novel SARS-CoV-2 vaccine platforms: the Pfizer/BioNTech BNT162b2 and Moderna mRNA-1273 mRNA vaccines and the AstraZeneca ChadOx1/AZD1222 and Janssen Ad.26COV2.S vaccines. After final immunization, antibody profiles were compared in naive individuals (without prior SARS-COV-2 infection) and those with previous SARS-CoV-2 infection (hybrid immunity). Striking differences were noted in the functional humoral immune response between mRNA and vectored vaccines in the naive population that were linked to differences in protective immunity between vaccine platforms. Moreover, we observed significant increases in the magnitude and quality of the hybrid immune response across different vaccines, marked by a unique, selectively expanded, S2-specific effector antibody response in the setting of hybrid immunity. Given the greater conservation in S2 across VOCs and across additional coronaviruses, this uniquely expanded S2-specific functional humoral immune response may represent a key mechanism that provides enhanced real-world efficacy against severe disease and death. Thus, next-generation vaccines able to promote enhanced functional S2-specific humoral immunity may provide enhanced protection against severe disease and death.

RESULTS

Characteristics of the four vaccine cohorts

Serum samples from adults with and without prior SARS-CoV-2 infection who followed a complete immunization schedule using one of the four available SARS-CoV-2 vaccines were analyzed. Patients received either two doses of either of the mRNA vaccines, (1) BNT162b2 (Pfizer; vaccination only, n = 35; hybrid immunity, n = 9) or (2) mRNA-1273 (Moderna; vaccination only, n = 19; hybrid immunity, n = 1), (3) one dose of the Ad26-vectored vaccine Ad26.COV2.S (Janssen; vaccination only, n = 25; hybrid immunity, n = 8), or (4) two doses of the ChAdOx-vectored vaccine AZD1222 (AstraZeneca; vaccination only, n = 19; hybrid immunity, n = 3). Blood was collected after final immunization at medians of 8, 8, 34, and 7 days from the final dose, at a time of presumed peak plasmablast expansion, respectively. The demographic characteristics of the four groups of vaccinees are provided in Table S1. The median age of the different cohorts was between 35 and 60 years old, with ages ranging from 21–77 years. For the vaccines including two doses in the primary immunization series (Pfizer, Moderna, and AstraZeneca), the median time between doses was 3 or 4 weeks for Pfizer and Moderna, respectively, and 66 days for the AstraZeneca vaccine, reflecting the policy in the United Kingdom, where the vaccinees resided.

mRNA and vector SARS-CoV-2 vaccines trigger functionally divergent antibody profiles

Despite the fact that mRNA and vector SARS-CoV-2 vaccines each induce antibody titers and neutralizing antibodies,[5,11,33,34] significant differences have been noted between these vaccine platforms,[35] in part attributable to divergent antibody levels. Despite the greater mRNA vaccine efficacy reported in early trials, the real-world effectiveness of the vaccines declined for mRNA Pfizer/BNT16b2 and Moderna mRNA-1273 as well as vector DNA Ad26.COV2.S and AZD1222 vaccines[5,6] as VOCs spread globally.[36,37] This leads to the hypothesis that differences beyond the overall levels of antibodies could explain efficacy differences among the vaccines. Thus, we performed comprehensive antibody profiling across four groups of vaccinees against the original D614G spike antigen (wildtype [WT]) in naive individuals after immunization (Figure 1A). Antibody profiles were interrogated against the full spike as well as the S1 domain, S2 domain, receptor-binding domain (RBD), and N-terminal domain (NTD). Striking differences were observed in vaccine-induced antibody profiles across the four vaccine platforms (Figures 1B and S1), marked by lower overall titers and functionality in the vector vaccine platforms and robust functionality and antibody levels in mRNA-1273- and BNT162b2-immunized individuals. Univariate comparison of spike-specific antibody levels across the vaccine platforms highlighted the expected elevated levels of immunoglobulin G1 (IgG1), IgG2, IgG3, IgA, and IgM responses triggered by the mRNA vaccines compared with the vector vaccines (Figure 1C). Additionally, higher IgA and IgM responses were observed in mRNA-1273 vaccinees than in BNT162b2 recipients. Similarly, Ad26.COV2.S vaccine recipients exhibited higher IgA and IgM levels compared with individuals who received the entire course of the AZD1222 vaccine. These data point to mRNA/vector and within-platform differences in antibody profiles.

To begin to capture other functional differences in vaccine-induced humoral profiles, we next compared the Fcγ receptor (FcγR) binding profiles of SARS-CoV-2-specific antibodies after immunization for each group. Robust FcγR-binding antibodies were observed for mRNA vaccinees, marked by significantly higher levels of Fcγ2A, Fcγ2B, and Fcγ3B binding in mRNA-1273 vaccinees compared with BNT162b2 recipients. Moreover, both vector-induced spike-specific antibodies bound to the activating opsonophagocytic Fcγ2A receptor, but neither induced appreciable levels of Fcγ3A- or Fcγ3B-binding antibodies. Conversely, AZD1222 recipients elicited slightly higher levels of inhibitory Fcγ2B-binding antibodies compared with Ad26.COV2.S recipients (Figure 1D), pointing to significant differences across

CellPress
OPEN ACCESS

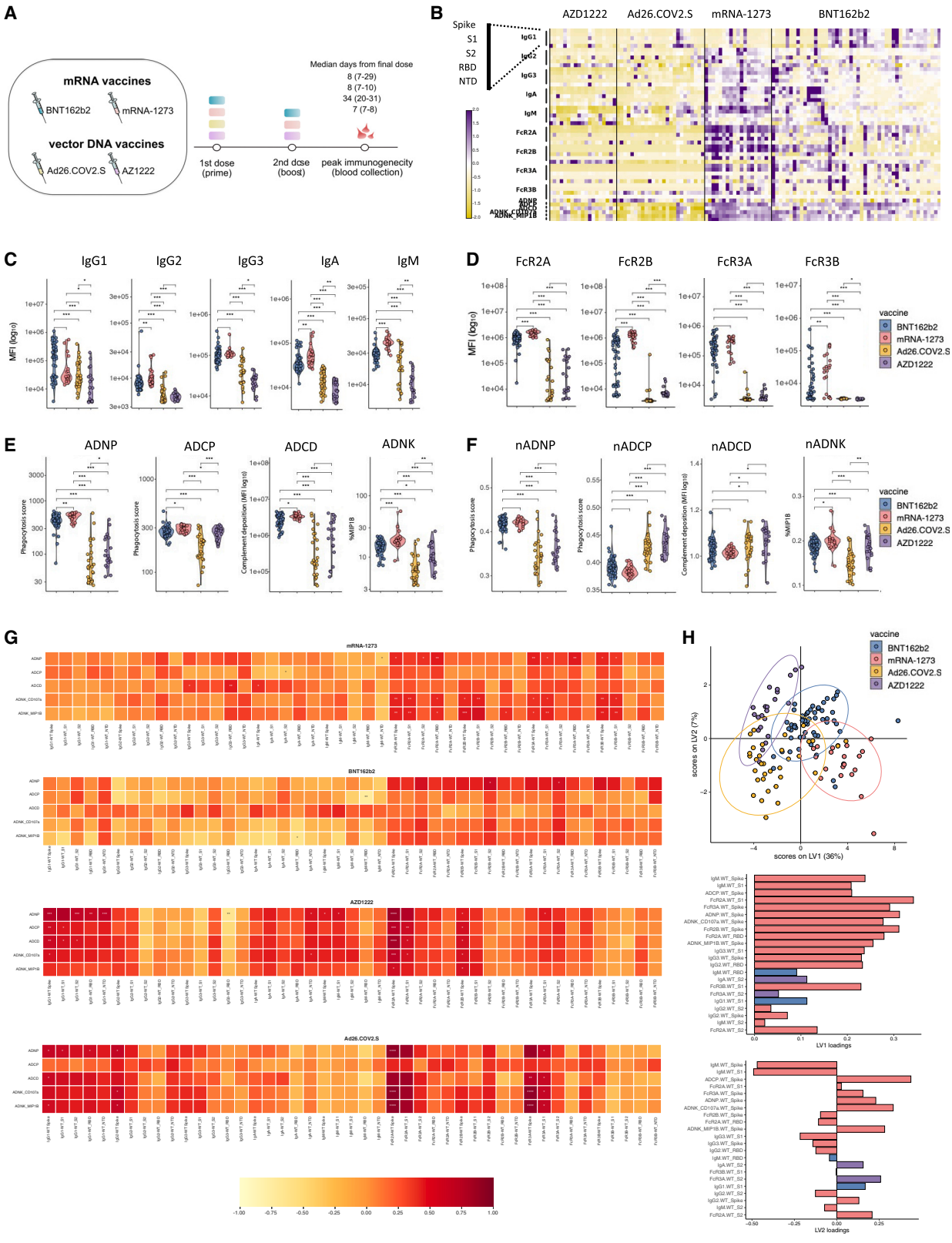

(legend on next page)

mRNA/vector platforms as well as within platforms in FcR binding profiles.

To determine whether the differences in FcR binding translated to functional differences, we next compared several Fc-mediated effector activities of vaccine-induced antibodies (Figure 1E). As expected, mRNA vaccines induced more robust spike-specific antibody-dependent neutrophil phagocytosis (ADNP), antibody-dependent cellular phagocytosis (ADCP), antibody-dependent complement deposition (ADCD), and antibody-dependent natural killer (ADNK) activation activity. Within the mRNA vaccines, mRNA-1273 vaccinees exhibited the highest ADNP and ADNK activity. Additionally, between the vectored vaccines, AZD1222 triggered superior ADCP and ADNK activity compared with Ad26.COV2.S vaccination, highlighting differences between and within platforms.

However, given the striking differences in titers (Figure 1C) and FcR (Figure 1D) binding levels and the less pronounced differences in antibody effector functions across the platforms (Figure 1E), we next aimed to define the relationship of antibody levels to antibody effector function. Specifically, spike-specific antibody functions were normalized to spike-specific IgG levels to capture the functionality per antibody quality induced by each vaccine platform. Strikingly, normalization of ADNP, ADCP, ADCD, and ADNK to a total spike-specific IgG level (Figure 1F) revealed preferential induction of more ADNP- and ADNK-inducing antibodies by the mRNA platforms. Conversely, ADCP and ADCD were induced more effectively, on a per-antibody level, by the vectored vaccines. Thus, on a per-antibody level, distinct vaccine platforms may provide precise instructions to the evolving B cell immune response to elicit specific functional activities that may be differentially controlled at the level of different isotype/subclass selection or Fc glycosylation.

We next aimed to define the epitope-specific functional response across the vaccine platform. Specifically, the relationships between spike-specific antibody functions and SARS-CoV-2 WT spike-, S1-, S2-, RBD- and NTD-specific antibody levels and FcγR binding were investigated (Figure 1G). Interestingly, IgG1 levels were strongly associated with antibody functions in mRNA-1273- and Ad26.COV2.S-immunized individuals. Conversely, FcR binding levels were tightly associated with antibody effector function in BNT162b2 vaccinees in addition to mRNA-1273 and Ad26.COV2.S vaccinees. Conversely, a more diffuse response was observed in AZD1222 vaccinees, with an interesting, stronger immunodominant relationship of S2-specific FcR binding associated with several antibody functions. Finally, IgA and IgM responses were solely associated with antibody effector functions in Ad26.COV2.S-immunized individuals, pointing to striking differences in the overall architecture of the humoral immune response among the four vaccines.

Thus, to gain an overall appreciation for whether the vaccine profiles differ from one another, we finally integrated all the humoral data for each vaccine group and used least absolute shrinkage and selection operator (LASSO) to conservatively reduce the overall features to the minimal number of vaccine measurements that could discriminate between all four coronavirus disease 2019 (COVID-19) vaccine-induced profiles after final immunization (Figure 1H). The data were then visualized using a partial least-squares discriminant analysis (PLS-DA). Latent variable 1 (LV1) separated vectored (left) and mRNA vaccines (right) from one another. Conversely, LV2 split the vaccines within the platforms, with BNT162b2 and AZD1222 segregating together (top), and mRNA-1273 and Ad26.COV2.S segregating together (bottom). The latent space loading bar graphs illustrate the minimal features that drove the separation between the vaccine profiles, marked by enhanced spike- and S1-specific IgM-, Fcγ2A-, and Fcγ2B-binding antibodies and effector functions such as ADCP, ADNP, and ADNK in mRNA-vaccinated individuals. Conversely, RBD-specific IgM and S1-specific IgG1 were enriched in the vectored vaccines. Separation across the platforms was more nuanced, marked by enhanced ADCP, FcγR3a, ADNP, NK cell, and S2-specific FcγR2a binding in BNT162b2 and AZD1222 but more spike-specific IgM, FcγR2b, RBD-specific, IgG3, and S2-specific Ig FcγR2A in mRNA-1273 and Ad26.COV2.S vaccinees. Thus, mRNA vaccination was marked by an overall magnitude increase in the functional quality of the humoral immune response, but differences in overall functionality and epitope specificity appeared to drive within-platform

Figure 1. mRNA and vector DNA SARS-CoV-2 vaccines trigger functionally divergent antibody profiles

(A) Schematic of the study groups. Individuals received two doses of mRNA vaccine BNT162b2 (n = 48, blue) or mRNA-1273 (n = 19, pink), one dose of the vector DNA Ad26.COV2.S vaccine (n = 25, yellow), or two doses of the vector DNA vaccine AZD1222 (n = 19, violet). Blood was collected after the final immunization time point (with a median of 8, 8, 34, and 7 days from the final dose, respectively).

(B) The heatmap summarizes the SARS-COV-2 WT spike-, S1-, S2-, RBD-, and NTD-specific IgG1, IgG2, IgG3, IgA1, and IgM titers as well as the ability of the SARS-CoV-2-specific antibodies to bind to the low-affinity FcγRs (FcγR2A, FcγR2B, FcγR3a, and FcγR3b) across individuals who received a mRNA (BNT162b2 or mRNA-1273) or vector DNA (Ad26COV2.S or AZD122) vaccine after the final immunization. Each column represents a different individual. Each row represents a distinct feature that was analyzed.

(C–F) Univariate comparisons of WT spike-specific (C) IgG1, IgG2, IgG3, IgA, and IgM; (D) FcγR2A, FcγR2B, FcγR3A, and FcγR3B binding levels; and (E) functional properties, such as ADNP, ADCP, ADCD, and ADNK across recipients of four different COVID-19 vaccine platforms. The antibody-mediated effector functions were normalized to total IgG antibody level to highlight the effector properties of antibodies triggered by different COVID-19 vaccines independent of antibody level (F). Each dot represents a mean of technical replicates or biological replicates (for functional assays) for each single individual. Differences were defined using a Mann-Whitney U test, and all p values were corrected for multiple testing correction using the Benjamini-Hochberg (BH) method: ***$p < 0.001$, **$p < 0.01$, *$p < 0.05$.

(G) Partial least-squares discriminant analysis (PLS-DA) was used to visualize the separation between the COVID-19 vaccine platform based on the LASSO selected features. Each dot represents an individual vaccinee within the group. The bar graph shows the latent vector (LV) loadings of the LASSO-selected features in LV1 and LV2.

(H) The correlation heatmap shows Spearman correlation coefficients between the antibody-mediated effector functions and SARS-CoV-2 WT spike, S1, S2, RBD, and NTD antibody level and FcR binding properties after final immunization across four different COVID-19 vaccine platforms. Negative correlations are indicated in yellow-orange, and positive correlations are shown in red.

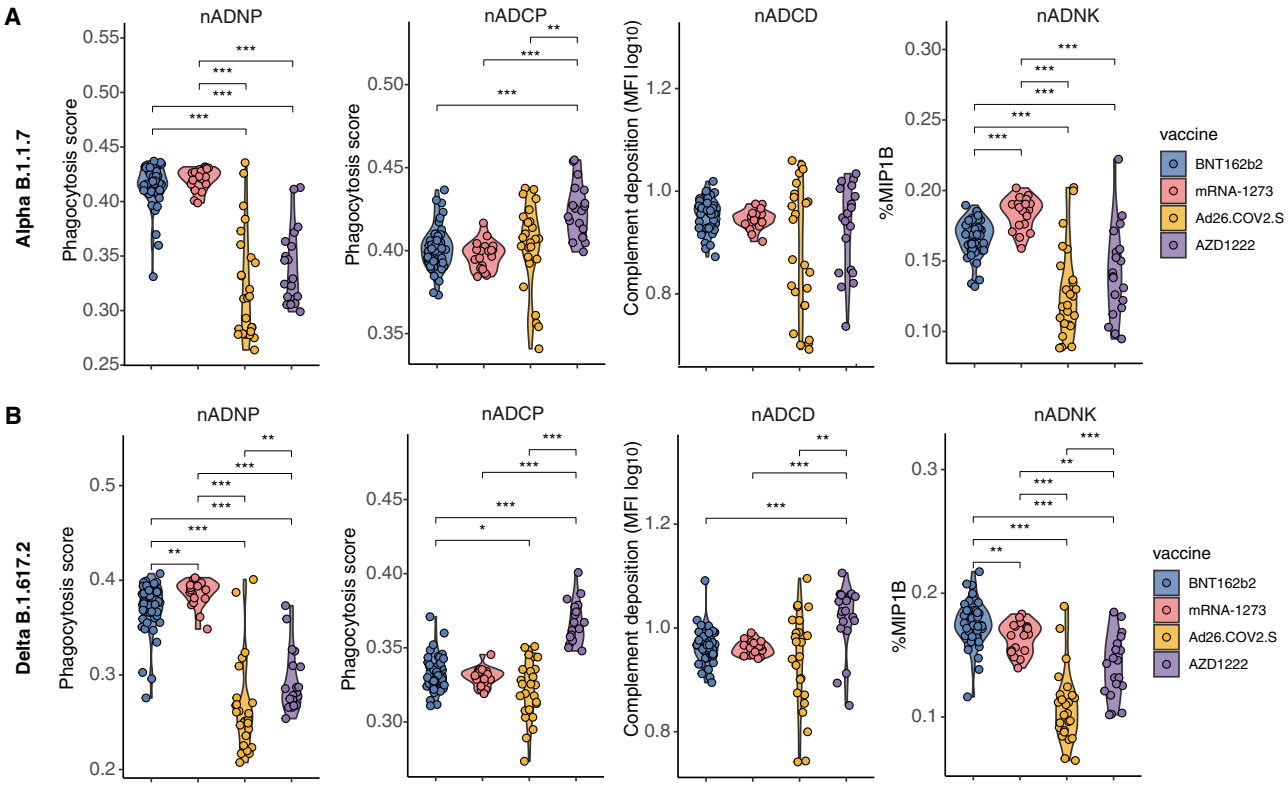

Figure 2. mRNA and vector DNA SARS-CoV-2 vaccines induce cross-reactive functional antibodies across VOCs

(A and B) Violin plots showing univariate comparisons of ADNP, ADCP, ADCD, and ADNK of (A) B.1.1.7 and (B) B.1.617.2 SARS-CoV-2 VOC spike-specific antibodies normalized by the total IgG antibody level across four different COVID-19 vaccine platforms. Each dot represents a mean of two biological replicates for each single individual. Differences were defined using Mann-Whitney U test, and all p values were corrected for multiple comparisons using the BH method: ***$p < 0.001$, **$p < 0.01$, *$p < 0.05$.

differences in antibody profiles, which may help explain differences in real-world efficacy differences in the setting of emerging VOCs.

Cross-vaccine antibody functional differences across VOCs

Despite the emergence of several VOCs that led to enhanced transmission because of neutralization escape, little is known about the functional quality of vaccine-induced antibodies with respect to VOCs. Thus, we next profiled the per-antibody vaccine-induced functional profile across the Alpha (B.1.1.7) and Delta (B.1.617.2) VOC spikes (Figure 2). Similar to the profiles observed for the D614G spike, on a per-antibody level, mRNA vaccines induced higher ADNP and ADNK activity, but mRNA-1273 induced slightly higher ADNK-activating antibodies compared with BNT162b2 (Figure 2A). Conversely, ADCP and ADCD were higher on a per-antibody level in the vectored vaccines than in the mRNA vaccines, with AZD1222 inducing more elevated levels of ADCP-inducing antibodies compared with Ad26.COV2.S vaccination.

Interestingly, the profiles of the Delta variant were distinct (Figure 2B), marked by higher levels of ADNP induced by mRNA-1273 but higher levels of ADNK driven by BTN126b2, although both ADNP and ADNK were higher in mRNA vaccinees. For ADCP and ADCD, the profile was slightly different, with only AZD1222 inducing the highest levels of these opsonophagocytic functions compared with the other three platforms, pointing to significant differences in functional humoral vaccine performance across VOCs.

Characteristics of the hybrid immunity and vaccination-only cohorts

Vaccination after natural SARS-CoV-2 infection, known as hybrid immunity, has been shown to increase the potency and breadth of humoral responses to SARS-CoV-2[23,24] and lead to enhanced real-world efficacy against VOCs.[21,22] However, it is unclear whether hybrid immunity can alter the functional quality of the humoral immune response. Thus, we next compared the cohort of individuals without prior SARS-CoV-2 infection (hereafter called "vaccination only") with those with prior natural SARS-CoV-2 infection (hereafter called "hybrid immunity") who received (1) mRNA vaccines, including BNT162b2 (vaccination only n = 35, D1 n= 35, D2 = 48; and hybrid immunity n = 9, D1 = 9, D2 = 9; D1, number of dose 1 vaccinees; D2, number of dose 2 vaccinees) and mRNA-1273 (vaccination only n = 19, D1 = 19, D2 = 19; and hybrid immunity D1 = 1, D2 = 1), or (2) received either of the vectored vaccines, including Ad26.COV2.S after the first dose (vaccination only n = 25, and hybrid immunity

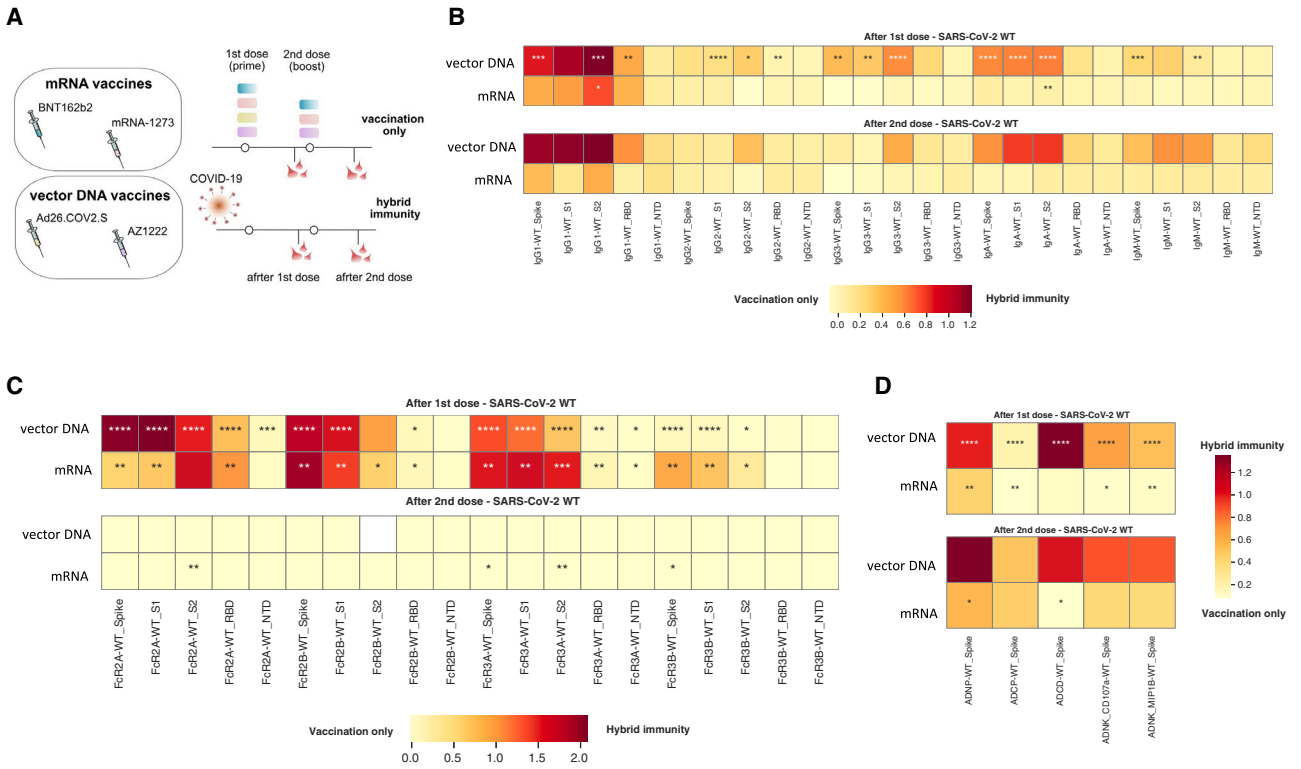

Figure 3. SARS-CoV-2 infection prior to one or two doses of a mRNA and vector DNA vaccine enriches the functional S2-specific antibody profile compared with vaccination only

(A) Schematic of the study groups. Individuals without (n = 98) and with prior COVID-19 (n = 21) received two doses of mRNA vaccine BNT162b2 (vaccination only, n = 35; hybrid immunity, n = 9; blue) or mRNA-1273 (vaccination only, n = 19; hybrid immunity, n = 1; pink), one dose of the vector DNA Ad26.COV2.S vaccine (vaccination only, n = 25; hybrid immunity, n = 8; yellow), or two doses of the vector DNA vaccine AZD1222 (vaccination only, n = 19; hybrid immunity, n = 3; violet). Blood was collected after the first and second dose of a vaccine.

(B–D) Heatmaps show the median delta value (Δ) in log10 scale between vaccination only and hybrid immunity for SARS-CoV-2 spike-, S1-, S2-, RBD- and NTD-specific (B) IgG1, IgG2, IgG3, IgA, and IgM level; (C) FcγR2A, FcγR2B, FcγR3A and FcγR3B binding levels; as well as (D) SARS-CoV-2 WT spike-specific ADNP, ADCP, ADCD, and ADNK after the first and second dose of four different COVID-19 vaccines. Each sample was run in technical duplicates (for antibody level and FcγR binding) or biological replicates (for functional assays). Differences were defined using a Mann-Whitney U test, and all p values were corrected for multiple comparisons using the BH method: ***p < 0.001, **p < 0.01, *p < 0.05.

n = 8) and AZD1222 after (vaccination only n = 19, D1 = 30, D2 = 19; and hybrid immunity n = 3, D1 = 9, D2 = 3) (Figure 3A). Profiles were assessed after the first and second dose of the vaccines.

Heatmaps were constructed using the SARS-CoV-2-specific antibody profiles depicting the median delta differences between individuals who only received the vaccine or who had hybrid immunity across vector and mRNA vaccines (Figures 3B–3D), with dark blue indicating larger differences between groups (Figures 3B–3D). As expected, we observed enhanced augmentation of immunity after the first dose in individuals who received a vectored vaccine (Figure 3B). Moreover, among the features, only two features in the mRNA vaccine-induced immune response were significantly augmented in individuals with hybrid immunity, related to S2-specific IgG1, IgG3, and IgA levels. Interestingly, several antibody levels increased again in the vectored vaccinees after the second immunization, with a preferential, albeit not statistically significant, enrichment in S1 and S2 IgG1 and IgA responses. A trend toward non-significant enrichment of spike/S2-specific IgG1 was again observed in mRNA vaccinees with hybrid immunity. These data pointed to a more dramatic impact of hybrid immunity among vectored vaccinees gaining IgG1, IgG3, and IgA immunity and a selective increase in S2-specific immunity with mRNA vaccination.

To further define the functional impact of hybrid immunity, we next examined the differences in vaccine-induced FcR-binding antibodies in individuals with hybrid immunity compared with the naive population. Surprisingly, distinct from antibody isotype/subclass-level changes, significant augmentations were observed in FcR binding profiles across individuals who received a vector or mRNA vaccine (Figure 3C). Specifically, after the first dose, individuals who received a vectored vaccine experienced a strikingly significant rise in spike-, S1-, and S2-specific FcγR2a, FcγR2b, and FcγR3a, and a significant but more limited augmentation in FcγR3b-binding antibodies. Interestingly, mRNA vaccinees also experienced significant augmentation in spike-, S1-, S2-, and RBD-specific FcγR2a, FcγR2b, FcγR3a, and FcγR3b binding after the first dose. Additional significant although smaller improvements were noted in NTD-specific FcR binding in vectored volunteers. However, despite this remarkable improvement in functionality, no differences were noted in FcR binding

CellPress
OPEN ACCESS

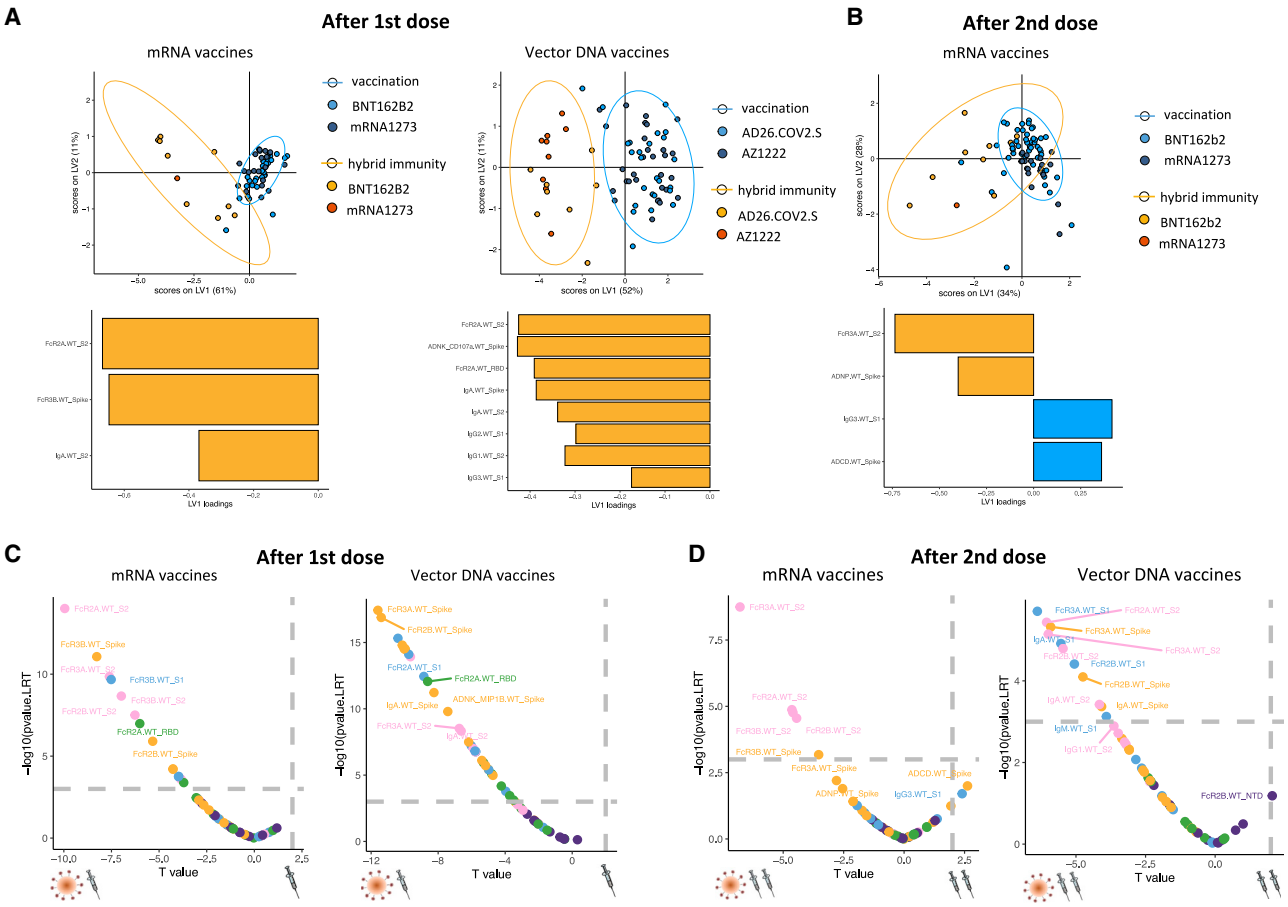

Figure 4. SARS-CoV-2 infection prior to one or two doses of mRNA and vector DNA vaccine induces specific unique features of the humoral immune response

(A and B) PLS-DA was used to visualize the separation between vaccination only and hybrid immunity for mRNA and vector DNA vaccinees after the (A) first and (B) second dose based on the WT SARS-CoV-2 LASSO-selected features. Blue dots represent vaccination only for either BNT162b2 or AD26.COV2.S (light blue) and mRNA-1273 or AZD1222 (dark blue); yellow dots represent hybrid immunity for either BNT162b2 or AD26.COV2.S (light yellow) and mRNA-1273 or AZD1222 (orange). Each dot represents an individual vaccinee within the group. The bar graph shows the latent vector (LV) loadings of the LASSO-selected features in LV1 and LV2; blue for vaccination only and yellow for hybrid immunity.

(C and D) Volcano plots of pairwise comparisons across vaccination only and hybrid immunity for vector DNA and mRNA vaccines after the first (C) and second dose (D) were controlled for age and sex of individuals. The x axis represents the *t* value of the full model, and the y axis denotes the p values by likelihood ratio test comparing the null model and full model. The null/full model represents the association between each individual measurement (response) and all collected demographic information (STAR Methods). The horizontal gray dashed line denotes p = 0.05, and the vertical gray dashed line denotes a manually selected threshold (*t* = 2). Each sample was run in technical duplicates (for antibody level and FcγR binding) or biological replicates (for functional assays).

after the second dose of vaccination in the hybrid immunity group across the different vaccine platforms, suggesting that hybrid immunity may only afford an advantage in FcR binding after the first dose of immunization.

However, to define whether hybrid immunity may modulate antibody effector function, we compared differences in antibody function after the first and second dose of the vaccines (Figure 3D). After the first dose, a substantial enhancement was observed in all functions in vector-immunized individuals, with the strongest augmentation in spike-specific ADCD activity. spike-specific ADNP, ADCP, and ADNK were also significantly increased in mRNA vaccinees after a single dose of the vaccine. Interestingly, after the second dose, individuals who received a vector still experienced a trend toward a large augmentation in ADNP, ADCD, and ADNK activity, suggesting that, even after a second dose, individuals with hybrid immunity may harbor more robust antibody functionality to SARS-CoV-2 compared with individuals who received vectored vaccines alone. Interestingly, despite the fact the fold increase was smaller, hybrid immunity also showed increased levels of ADNP and ADCD among mRNA-vaccinated individuals after the second dose, again pointing to potentially enhanced opsonophagocytic protection that may contribute to the improved real-world effectiveness observed in the setting of the previous infection.

To gain a more profound sense of the specific unique features of the humoral immune response induced by hybrid immunity, we performed a multivariate LASSO/PLS-DA analysis (Figures 4A and 4B). Near-complete separation was observed between

individuals with hybrid immunity compared with those solely vaccinated with either an mRNA (Figure 4A) or a vector (Figure 4B) vaccine. Interestingly, only four of a total of 40 features analyzed for each sample were sufficient to separate mRNA vaccinees with hybrid immunity or not. These features included selective enrichment of S2-specific antibodies binding to FcγR3A and spike-specific ADNP in hybrid immunity compared with higher S1-specific IgG3 and spike-specific ADCD among vaccinated-only individuals (Figure 4C). Conversely, hybrid immunity led to highly significant enrichment of multiple FcR, IgA, and IgG1/2/3 responses in vector immunity, with a notable increase in S2-specific FcγR2a, IgG1, and IgA. After the second dose, mRNA vaccinee profiles continued to exhibit unique profiles in individuals with hybrid immunity, marked again by selective augmentation of S2-specific FcγR2a and IgA and higher levels of spike Fc of S2-specific antibodies binding to FcγR3A and spike-specific ADNP FcγR3b (Figure 4D). Furthermore, paired, nested, mixed linear models were used to rank the features that differed most across hybrid and naive immune profiles (Figure 4G), highlighting the presence of S2-specific FcR-binding antibodies as top predictors of hybrid immunity following a single or double dose of mRNA vaccination as well as among the top enriched features in hybrid immunity following a double dose of vector vaccination. Hybrid immunity did augment the overall spike-specific response following vector vaccination. Thus, these data argue that hybrid immunity extends the overall spike-specific response following vectored immunity but selectively augments S2-specific immune responses following mRNA vaccination, potentially pointing to a breach of vaccine-induced immunodominance that shifts the response to highly conserved regions of spike that may confer additional non-neutralizing protection against VOCs.

SARS-CoV-2 infection prior to one or two doses of mRNA and vector COVID-19 vaccines improves the functional breadth of SARS-CoV-2 VOC responses

Emerging data suggest that hybrid immunity may also expand the breadth of immunity to additional VOCs.[23,25–27] Given the unique expansion of S2 response observed with hybrid immunity, we next aimed to profile the overall landscape of antibody levels (Figure 5A), FcR binding profiles (Figure 5B), and functions (Figure 5C) across the mRNA and vectored vaccines. Focusing on the Beta, Delta, and Omicron BA.1.1.529 and BA.5 VOCs, we observed a significant expansion of Beta, Delta, and Omicron BA.1.1.529 and BA.5 spike-specific responses in hybrid vector-immunized individuals, with augmentation, albeit non-significant, in the Beta and Omicron BA.1.1.529 RBD and lesser but significant augmentation in Delta and Omicron BA.5 RBD-binding IgG1 levels, suggesting that the majority of hybrid-induced antibody responses may be directed outside of the RBD. Interestingly, hybrid immunity after the first dose of the vector vaccines was also accompanied by an increase in IgA responses, pointing to a broader enhancement of immunity. This augmentation was less substantial in hybrid-immune individuals after the first dose of mRNA vaccination, although significant increases were noted in IgG1 responses to Delta, Omicron BA.1.1.529, and BA.5 spikes and the Omicron BA.5 RBD. Moreover, after the second dose, a limited increase in Beta and Delta IgG1 binding as well as Omicron BA.1.1.529 and BA.5 was noted in hybrid-immune individuals after receiving vector and mRNA vaccination, respectively. However, the differences were not statistically significant.

In contrast to the less robust increases in antibody/isotype titers, a highly significant increase in FcγR-binding antibodies was noted across both platforms after the first immunization in hybrid-immune individuals, marked by higher levels of FcR2A-, FcR2B-, and FcR3A-binding antibodies to Beta, Delta, and Omicron BA.1.1.529 spike and a few RBD antigens. Similar potent augmentation was observed in hybrid-immune individuals after the first dose of mRNA vaccination, highlighting the preferential increase in FcγR-binding antibodies to whole spike VOC antigens (Figure 5B). Similarly, functional profiling across VOCs pointed to an overall significant expansion of all antibody functions following a single vector vaccination (Figure 5C), most dramatically observed for ADCD and ADNP. However, a single dose of mRNA vaccination also drove enhanced functionality, particularly ADNP activity, in individuals who were infected previously. Even a second dose of vectored vaccination further enhanced ADNP and ADCD to the Beta spike. Conversely, more limited functional augmentation was observed with the second dose of mRNA vaccination, but the augmentation was significant for ADNP and ADCD. Thus, these data suggest that hybrid immune augmentation of particular antibody effector functions across VOCs may contribute to enhanced control and clearance of the infection and, ultimately, persistent attenuation of disease in the setting of neutralization escape.

In summary, here we highlighted Fc profile differences across mRNA vaccines as well as adenoviral vector vaccines, in addition to recapitulating previously observed differences in neutralizing antibody levels and binding antibody titers between vaccine platforms. Despite the lower antibody titers induced by vectored vaccines, similar functional opsonophagocytic functions were induced at a per-antibody level, potentially conferring currently unappreciated higher levels of protection against VOCs via non-neutralizing antibody mechanisms. Moreover, while the platforms benefitted from hybrid immunity at differential levels, all platforms led to augmented S2-specific immunity that may play an essential role in VOC-mediated non-neutralizing control and attenuation of disease.

DISCUSSION

The COVID-19 pandemic led to a revolution in vaccine development, resulting in large-scale testing of several novel vaccine platforms and adjuvants in response to this rapidly spreading and often unpredictable pathogen. This near head-to-head testing of novel vaccines highlighted differences in efficacy induced by distinct platforms.[9,38–40] However, as the pandemic evolved, waning immunity and the evolution of neutralization-resistant VOCs challenged the assumed correlates of protection because neutralizing antibody titers were no longer a robust predictor of protection against severe COVID-19. Instead, transmission increased globally in the absence of a concomitant rise in severe disease and death in vaccinated populations, suggesting that other aspects of the vaccine-induced humoral immune response are likely to be key to protection against disease. Differences in neutralizing titers have not reliably predicted

CellPress
OPEN ACCESS

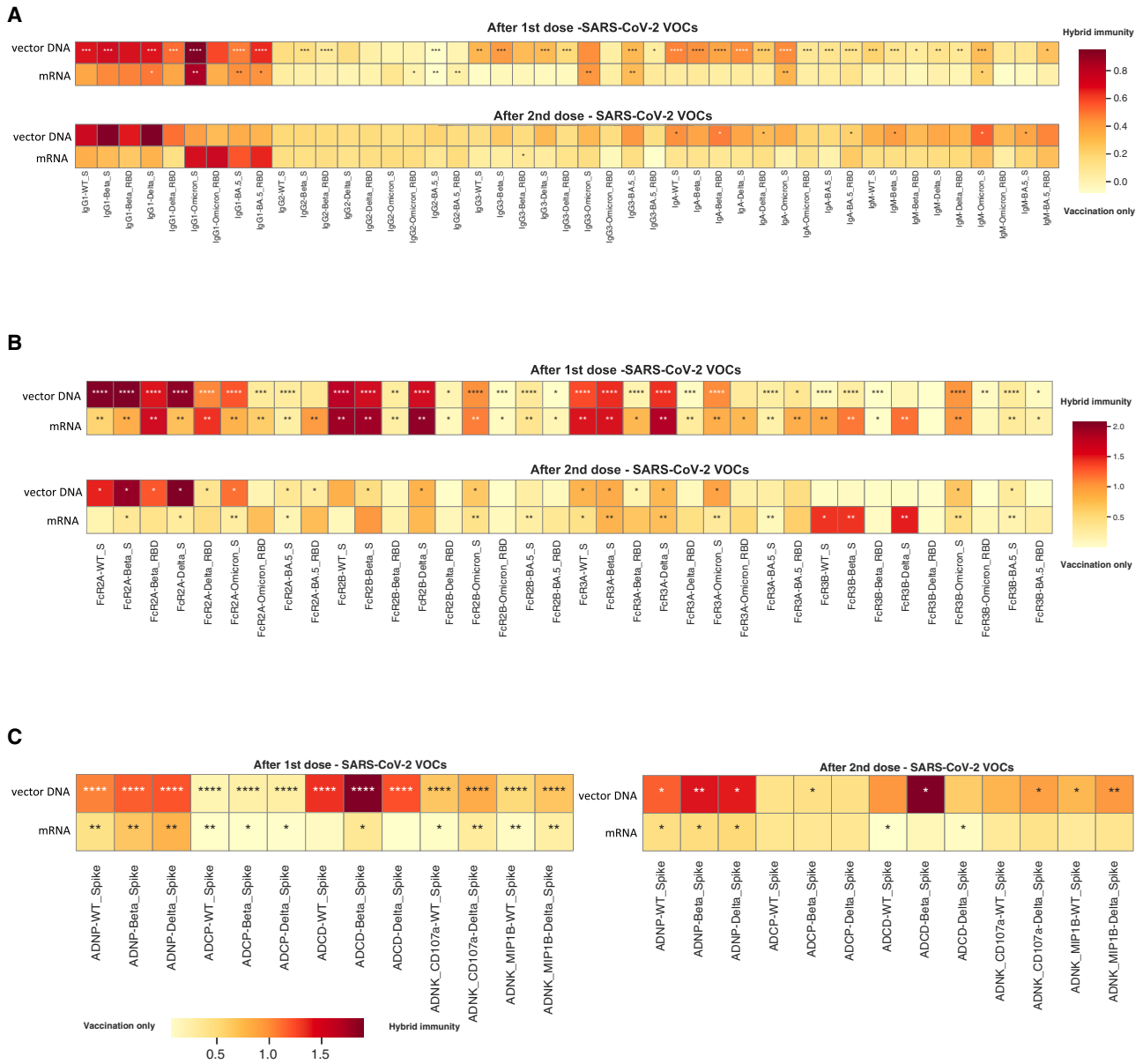

Figure 5. SARS-CoV-2 infection prior to one or two doses of a mRNA and vector DNA vaccine improves the functional breadth of SARS-CoV-2 VOC antibody response

(A–C) Heatmaps showing the median delta value (Δ) in log10 scale between vaccination only and hybrid immunity for SARS-CoV-2 WT, Alpha B.1.1.7, Beta B.1.351, Delta B.1.617.2, Omicron B.1.1.529, and BA.5 spike- and RBD-specific (A) IgG1, IgG2, IgG3, IgA, and IgM level; (B) FcγR2A, FcγR2B, FcγR3A, and FcγR3B binding levels; as well as (C) SARS-CoV-2 WT and Beta B.1.351 and Delta B.1.617.2 spike-specific ADNP, ADCP, ADCD, and ADNK after the first and second dose of four different COVID-19 vaccines. Each sample was run in technical duplicates (for antibody level and FcγR binding) or biological replicates (for functional assays). Differences were defined using a Mann-Whitney U test, and all p values were corrected for multiple comparisons using the BH method: ***$p < 0.001$, **$p < 0.01$, *$p < 0.05$.

discrepancies in real-world effectiveness between mRNA vaccines.[36,37] Antibody levels and T cell immune responses, robustly induced by vectored vaccines, have not been directly predictive of differences in vaccine efficacy.[41–43] Moreover, emerging real-world data pointed to the highest levels of efficacy against COVID-19 among individuals who had been infected with SARS-CoV2 prior to vaccination, termed hybrid immunity.[22,42,44] Identification of platform-specific immune programming differences and how these may be tuned by hybrid immunity offers a unique opportunity to define the immunologic correlates of protection to guide rational boosting and next-generation vaccine design against newly emerging VOCs.

Several studies have shown an association between antibody binding titers and neutralization with protection across phase3

SARS-CoV-2 vaccine trials[45,46] as well as clinical efficacy against primary infection with SARS-CoV-2 after vaccination,[13,16] suggesting that post-immunization antibody levels can serve as a measure for short-term protection across diverse vaccine platforms.[16,47,48] While it has been observed that vaccine-induced neutralizing antibodies decrease rapidly over time,[49–52] binding antibodies appear to be more durable,[52,53] potentially pointing to a role of non-neutralizing antibody functions in long-term protection against disease. Additionally, in the setting of VOCs able to evade neutralizing antibodies,[54–56] emerging data suggest that vaccine-induced antibodies continue to recognize VOC spike antigens, further arguing that additional vaccine-induced antibody mechanisms likely contribute to protection.[57–59] Despite our growing appreciation for the role of innate immune recruiting Fc effector antibody functions in the resolution of severe disease,[19,20] monoclonal therapeutic efficacy,[18] and survival after convalescent plasma therapy,[60] little is known about the differences in Fc effector functions across vaccine platforms and how they may evolve in the setting of hybrid immunity.

As expected, mRNA vaccines induce higher antibody titers, FcR binding profiles, and antibody effector function than vectored vaccines. However, even among the mRNA vaccines, differences were noted in the magnitude of the functional humoral immune response. Higher IgM and IgA responses were induced by mRNA-1273 and potentially linked to enhanced FcγR binding, ADNP, ADCP, ADCD, and ADNK, marking significant differences in antibody responses across SARS-CoV-2 mRNA vaccine platforms, potentially because of diversity in mRNA doses, intervals between vaccine injections, and lipid-nanoparticle formulation. Even across the adenoviral platforms, Ad26.CoV2.S induced higher titers compared with AZD1222 despite the fact that Ad26.CoV2.S was only administered as a single dose. Yet, AZD1222 induced higher FcγR2b binding antibodies as well as higher ADNP, ADCP, and ADNK activating antibodies compared with Ad26.CoV2.S, pointing to differences in the ability of distinct adenoviral vectors to drive diverse functional antibody profiles. Most surprising was the observation that normalization of antibody effector function by antibody titers pointed to higher-quality functional antibodies induced by vector vaccines compared with mRNA, with superior levels of ADCP and a trend toward higher ADCD induced by vectors compared with mRNA vaccines. However, the higher real-world efficacy of mRNA vaccines compared with vector DNA might suggest a cumulative effect of binding and functional antibodies responsible for protection from SARS-CoV-2. Whether this is related to the internal pattern recognition signal or innate cytokine responses induced by vectors compared with mRNA vaccines remains unclear. However, it may indicate the potential importance of using vectors as a prime or even as a boost in combination with mRNA vaccines in possible future heterologous vaccine strategies. The unique antibody functional profile generated by each vaccine is likely associated with the distinct inflammatory cues induced at the time of immunization, pushing T cell help and B cell responses toward specific class-switch recombination and Fc glycosylation profiles that collectively shape the overall FcγR binding and effector profiles of vaccine-induced polyclonal swarms of antibodies. Further dissection of these distinct signals may provide critical insights for future vaccine design efforts to elicit highly specialized antibody functional profiles to maximize disease protection.

Emerging real-world efficacy data suggest that vaccination following infection with SARS-CoV2 results in the greatest level of protection against severe COVID-19 disease.[22,42,44] This hybrid immune response quantitatively and qualitatively improved B cell and T cell responses.[61–63]

Even though the antibody titer was comparable after the first and second dose in hybrid immunity, whether infection shapes the durability of particular antibody responses over time remains unclear but can be addressed in long-term follow-up studies that have now been collected globally. Hybrid immunity led to a significant increase in S2-specific IgG and IgA titers for mRNA vaccines, pointing to selective expansion of immunity to the conserved portion of the spike antigen, with only trends in IgG1 titer and increases after the second dose of mRNA. Conversely, ADNP increased significantly after a first and second dose of mRNA vaccines in individuals with hybrid immunity, a function that has been specifically selectively enriched among survivors of severe COVID-19 and vaccinated macaques that resisted SARS-CoV-2 infection.[64] Moreover, after adjusting for demographics, S2-specific FγcR binding was selectively enriched among mRNA vaccinees with hybrid immunity but also observed following AZD1222 vaccination. The selective improvement of S2-specific immunity may point to two critical phenomena: (1) vaccination may promote largely immunodominant immunity to the S1 domain (including the RBD and NTD), whereas infection may help expand the response to the more conserved and less immunogenic S2 domain that is not as exposed, mainly in the stabilized spike antigens included in the mRNA vaccines; and (2) the expansion of immunity to the conserved S2 domain may be key to promoting cross-VOC immunity because of the higher conservation of S2 compared with other domains of the spike antigen.[65–67] Increased S2-specific antibodies able to mediate Fc effector functions have been observed previously among SARS-CoV-2 survivors[19,68] and in pre-pandemic children,[29] who are typically spared from SARS-CoV-2.[69,70] Because of their lower neutralizing potency,[71] S2-specific antibodies provide protection against disease in an Fc-dependent manner,[68] consistent with the mechanism by which hybrid immunity likely offers enhanced protection against VOCs. Specifically, the expansion of S2-specific responses with enhanced FcR binding likely promotes rapid capture and clearance of the virus after transmission. Because innate immune cells able to drive antibody-mediated clearance and killing are found more abundantly in the lower respiratory tract, these antibodies are unlikely to promote restriction in the upper respiratory tract but contribute to disease attenuation in collaboration with T cell immunity. Thus, given the structural conservation of the S2 domain as well as the neutralization and cross-reactive potential of S2 antibodies, the S2-specific response might reduce the influence of sequence-altering mutations and therefore could improve vaccine efficacy against seasonal circulating common cold coronaviruses and newly emerging VOCs.

Limitation of the study

There are some limitations to our study. We did not have large numbers of hybrid-immune subjects who received the mRNA-1273 and AZD1222 vaccines; thus, we were unable to look for

the impact of hybrid immunity in tuning specific vaccine platforms. Instead, we combined hybrid vaccinees who received an mRNA vaccine or DNA vaccine, given that the four-way PLS-DA clearly highlighted that the platforms contributed to the greatest amount of variation in antibody profiles (LV1). Future investigation based on individual platforms may reveal additional differences in hybrid immunity effects, given discrepancies in antigen stabilization or persistence following immunization. Additionally, this study was unable to address issues related to immune profiles over time. Yet, despite our results showing functionally divergent antibody profiles triggered by mRNA and adenovirus-vectored vaccine platforms in naive individuals, as well as the unique effect of hybrid immunity on expanding mRNA and vector vaccine-induced immunity to the conserved S2 domain. Moreover, future studies aiming to compare the impact of severity of COVID-19 prior to immunization as well as the impact of the interval from COVID-19 on shaping vaccine-induced immunity may provide further insights into opportunities to tune and improve immunity against SARS-CoV-2. Finally, larger, demographically controlled studies may provide further opportunities to define differences in vaccine-induced immune profiles that may account for real-world differences in efficacy. Nevertheless, these data highlight the unique programming effects across the vaccine platforms as well as the potentially critical importance of promoting functional humoral immunity to more conserved regions of betacoronaviruses, collectively pointing to new opportunities to develop next-generation COVID-19 vaccines or mix-and-match combinations able to drive the most effective immunity to existing and newly emerging VOCs.

STAR★METHODS

Detailed methods are provided in the online version of this paper and include the following:

- KEY RESOURCES TABLE
- RESOURCE AVAILABILITY
  - Lead contact
  - Materials availability
  - Data and code availability
- EXPERIMENTAL MODEL AND SUBJECT DETAILS
  - Description of the cohorts
  - Primary immune cells
  - Cell lines
- METHOD DETAILS
  - Luminex profiling
  - Effector functional assays
- QUANTIFICATION AND STATISTICAL ANALYSIS
  - Univariate comparison
  - Multivariate classification
  - Correlation analysis
  - Defining signatures of previous infection while also controlling for potential cofounders

SUPPLEMENTAL INFORMATION

Supplemental information can be found online at https://doi.org/10.1016/j.xcrm.2023.101048.

ACKNOWLEDGMENTS

We thank Nancy Zimmerman, Mark and Lisa Schwartz, an anonymous donor (financial support), Terry and Susan Ragon, and the SAMANA Kay MGH Research Scholars award for support. We acknowledge support from the Ragon Institute of Mass General, MIT, and Harvard (to G.A.) the Massachusetts Consortium on Pathogen Readiness (MassCPR) (to G.A.), and the National Institutes of Health (3R37AI080289-11S1, R01AI146785, U19AI42790–01, U19AI135995–02, U19AI42790-01, 1U01CA260476 – 01, and CIV-IC75N93019C00052) (to G.A.).

AUTHOR CONTRIBUTIONS

P.K., Y.D., D.G., and G.A. analyzed and interpreted the data. P.K. and J.S.-L.L. performed Luminex and functional assays. Y.D. performed the analysis. D.G. was responsible for all aspects of the clinical study and sample collection. P.K. and G.A. drafted the manuscript. All authors critically reviewed the manuscript.

DECLARATION OF INTERESTS

G.A. is a founder and equity holder of Seromyx Systems Inc., an employee and equity holder of Leyden Labs, and has received financial support from Abbvie, BioNtech, GSK, Gilead, Merck, Moderna, Novartis, Pfizer, and Sanofi. G.A.'s interests were reviewed and are managed by Massachusetts General Hospital and Partners HealthCare in accordance with their conflict-of-interest policies.

Received: June 13, 2022
Revised: December 13, 2022
Accepted: April 20, 2023
Published: May 16, 2023

REFERENCES

1. Hopkins University John Medicine Coronavirus Resource Center.
2. Nagy, A., and Alhatlani, B. (2021). An overview of current COVID-19 vaccine platforms. Comput. Struct. Biotechnol. J. *19*, 2508–2517. https://doi.org/10.1016/j.csbj.2021.04.061.
3. Baden, L.R., El Sahly, H.M., Essink, B., Kotloff, K., Frey, S., Novak, R., Diemert, D., Spector, S.A., Rouphael, N., Creech, C.B., et al. (2021). Efficacy and safety of the mRNA-1273 SARS-CoV-2 vaccine. N. Engl. J. Med. *384*, 403–416. https://doi.org/10.1056/NEJMoa2035389.
4. Polack, F.P., Thomas, S.J., Kitchin, N., Absalon, J., Gurtman, A., Lockhart, S., Perez, J.L., Pérez Marc, G., Moreira, E.D., Zerbini, C., et al. (2020). Safety and efficacy of the BNT162b2 mRNA Covid-19 vaccine. N. Engl. J. Med. *383*, 2603–2615. https://doi.org/10.1056/NEJMoa2034577.
5. Voysey, M., Clemens, S.A.C., Madhi, S.A., Weckx, L.Y., Folegatti, P.M., Aley, P.K., Angus, B., Baillie, V.L., Barnabas, S.L., Bhorat, Q.E., et al. (2021). Safety and efficacy of the ChAdOx1 nCoV-19 vaccine (AZD1222) against SARS-CoV-2: an interim analysis of four randomised controlled trials in Brazil, South Africa, and the UK. Lancet *397*, 99–111. https://doi.org/10.1016/s0140-6736(20)32661-1.
6. Sadoff, J., Gray, G., Vandebosch, A., Cárdenas, V., Shukarev, G., Grinsztejn, B., Goepfert, P.A., Truyers, C., Fennema, H., Spiessens, B., et al. (2021). Safety and efficacy of single-dose Ad26.COV2.S vaccine against Covid-19. N. Engl. J. Med. *384*, 2187–2201. https://doi.org/10.1056/NEJMoa2101544.
7. Oberhardt, V., Luxenburger, H., Kemming, J., Schulien, I., Ciminski, K., Giese, S., Csernalabics, B., Lang-Meli, J., Janowska, I., Staniek, J., et al. (2021). Rapid and stable mobilization of CD8(+) T cells by SARS-CoV-2 mRNA vaccine. Nature *597*, 268–273. https://doi.org/10.1038/s41586-021-03841-4.
8. Sahin, U., Muik, A., Vogler, I., Derhovanessian, E., Kranz, L.M., Vormehr, M., Quandt, J., Bidmon, N., Ulges, A., Baum, A., et al. (2021). BNT162b2 vaccine induces neutralizing antibodies and poly-specific T cells in

humans. Nature *595*, 572–577. https://doi.org/10.1038/s41586-021-03653-6.

9. Parry, H., Bruton, R., Stephens, C., Brown, K., Amirthalingam, G., Otter, A., Hallis, B., Zuo, J., and Moss, P. (2021). Differential immunogenicity of BNT162b2 or ChAdOx1 vaccines after extended-interval homologous dual vaccination in older people. Immun. Ageing *18*, 34. https://doi.org/10.1186/s12979-021-00246-9.
10. Moss, P. (2022). The T cell immune response against SARS-CoV-2. Nat. Immunol. *23*, 186–193. https://doi.org/10.1038/s41590-021-01122-w.
11. Amanat, F., Thapa, M., Lei, T., Ahmed, S.M.S., Adelsberg, D.C., Carreño, J.M., Strohmeier, S., Schmitz, A.J., Zafar, S., Zhou, J.Q., et al. (2021). SARS-CoV-2 mRNA vaccination induces functionally diverse antibodies to NTD, RBD, and S2. Cell *184*, 3936–3948.e10. https://doi.org/10.1016/j.cell.2021.06.005.
12. Kaplonek, P., Cizmeci, D., Fischinger, S., Collier, A.R., Suscovich, T., Linde, C., Broge, T., Mann, C., Amanat, F., Dayal, D., et al. (2022). mRNA-1273 and BNT162b2 COVID-19 vaccines elicit antibodies with differences in Fc-mediated effector functions. Sci. Transl. Med. *14*, eabm2311. https://doi.org/10.1126/scitranslmed.abm2311.
13. Khoury, D.S., Cromer, D., Reynaldi, A., Schlub, T.E., Wheatley, A.K., Juno, J.A., Subbarao, K., Kent, S.J., Triccas, J.A., and Davenport, M.P. (2021). Neutralizing antibody levels are highly predictive of immune protection from symptomatic SARS-CoV-2 infection. Nat. Med. *27*, 1205–1211. https://doi.org/10.1038/s41591-021-01377-8.
14. Cromer, D., Steain, M., Reynaldi, A., Schlub, T.E., Wheatley, A.K., Juno, J.A., Kent, S.J., Triccas, J.A., Khoury, D.S., and Davenport, M.P. (2022). Neutralising antibody titres as predictors of protection against SARS-CoV-2 variants and the impact of boosting: a meta-analysis. Lancet. Microbe *3*, e52–e61. https://doi.org/10.1016/s2666-5247(21)00267-6.
15. Folegatti, P.M., Ewer, K.J., Aley, P.K., Angus, B., Becker, S., Belij-Rammerstorfer, S., Bellamy, D., Bibi, S., Bittaye, M., Clutterbuck, E.A., et al. (2020). Safety and immunogenicity of the ChAdOx1 nCoV-19 vaccine against SARS-CoV-2: a preliminary report of a phase 1/2, single-blind, randomised controlled trial. Lancet *396*, 467–478. https://doi.org/10.1016/s0140-6736(20)31604-4.
16. Earle, K.A., Ambrosino, D.M., Fiore-Gartland, A., Goldblatt, D., Gilbert, P.B., Siber, G.R., Dull, P., and Plotkin, S.A. (2021). Evidence for antibody as a protective correlate for COVID-19 vaccines. Vaccine *39*, 4423–4428. https://doi.org/10.1016/j.vaccine.2021.05.063.
17. Bégin, P., Callum, J., Jamula, E., Cook, R., Heddle, N.M., Tinmouth, A., Zeller, M.P., Beaudoin-Bussières, G., Amorim, L., Bazin, R., et al. (2021). Convalescent plasma for hospitalized patients with COVID-19: an open-label, randomized controlled trial. Nat. Med. *27*, 2012–2024. https://doi.org/10.1038/s41591-021-01488-2.
18. Winkler, E.S., Gilchuk, P., Yu, J., Bailey, A.L., Chen, R.E., Chong, Z., Zost, S.J., Jang, H., Huang, Y., Allen, J.D., et al. (2021). Human neutralizing antibodies against SARS-CoV-2 require intact Fc effector functions for optimal therapeutic protection. Cell *184*, 1804–1820.e16. https://doi.org/10.1016/j.cell.2021.02.026.
19. Zohar, T., Loos, C., Fischinger, S., Atyeo, C., Wang, C., Slein, M.D., Burke, J., Yu, J., Feldman, J., Hauser, B.M., et al. (2020). Compromised humoral functional evolution tracks with SARS-CoV-2 Mortality. Cell *183*, 1508–1519.e12. https://doi.org/10.1016/j.cell.2020.10.052.
20. Atyeo, C., Fischinger, S., Zohar, T., Slein, M.D., Burke, J., Loos, C., McCulloch, D.J., Newman, K.L., Wolf, C., Yu, J., et al. (2020). Distinct early serological signatures track with SARS-CoV-2 survival. Immunity *53*, 524–532.e4. https://doi.org/10.1016/j.immuni.2020.07.020.
21. Pouwels, K.B., Pritchard, E., Matthews, P.C., Stoesser, N., Eyre, D.W., Vihta, K.D., House, T., Hay, J., Bell, J.I., Newton, J.N., et al. (2021). Effect of Delta variant on viral burden and vaccine effectiveness against new SARS-CoV-2 infections in the UK. Nat. Med. *27*, 2127–2135. https://doi.org/10.1038/s41591-021-01548-7.
22. Nordström, P., Ballin, M., and Nordström, A. (2022). Risk of SARS-CoV-2 reinfection and COVID-19 hospitalisation in individuals with natural and hybrid immunity: a retrospective, total population cohort study in Sweden. Lancet Infect. Dis. *22*, 781–790. https://doi.org/10.1016/s1473-3099(22)00143-00148.
23. Bates, T.A., McBride, S.K., Leier, H.C., Guzman, G., Lyski, Z.L., Schoen, D., Winders, B., Lee, J.Y., Lee, D.X., Messer, W.B., et al. (2022). Vaccination before or after SARS-CoV-2 infection leads to robust humoral response and antibodies that effectively neutralize variants. Sci. Immunol. *7*, eabn8014. https://doi.org/10.1126/sciimmunol.abn8014.
24. Wang, Z., Muecksch, F., Schaefer-Babajew, D., Finkin, S., Viant, C., Gaebler, C., Hoffmann, H.H., Barnes, C.O., Cipolla, M., Ramos, V., et al. (2021). Naturally enhanced neutralizing breadth against SARS-CoV-2 one year after infection. Nature *595*, 426–431. https://doi.org/10.1038/s41586-021-03696-9.
25. Stamatatos, L., Czartoski, J., Wan, Y.H., Homad, L.J., Rubin, V., Glantz, H., Neradilek, M., Seydoux, E., Jennewein, M.F., MacCamy, A.J., et al. (2021). mRNA vaccination boosts cross-variant neutralizing antibodies elicited by SARS-CoV-2 infection. Science *372*, 1413–1418. https://doi.org/10.1126/science.abg9175.
26. Doria-Rose, N.A., Shen, X., Schmidt, S.D., O'Dell, S., McDanal, C., Feng, W., Tong, J., Eaton, A., Maglinao, M., Tang, H., et al. (2021). Booster of mRNA-1273 strengthens SARS-CoV-2 Omicron neutralization. Preprint at medRxiv. https://doi.org/10.1101/2021.12.15.21267805.
27. Gruell, H., Vanshylla, K., Tober-Lau, P., Hillus, D., Schommers, P., Lehmann, C., Kurth, F., Sander, L.E., and Klein, F. (2022). mRNA booster immunization elicits potent neutralizing serum activity against the SARS-CoV-2 Omicron variant. Nat. Med. *28*, 477–480. https://doi.org/10.1038/s41591-021-01676-0.
28. Ebinger, J.E., Fert-Bober, J., Printsev, I., Wu, M., Sun, N., Prostko, J.C., Frias, E.C., Stewart, J.L., Van Eyk, J.E., Braun, J.G., et al. (2021). Antibody responses to the BNT162b2 mRNA vaccine in individuals previously infected with SARS-CoV-2. Nat. Med. *27*, 981–984. https://doi.org/10.1038/s41591-021-01325-6.
29. Gobbi, F., Buonfrate, D., Moro, L., Rodari, P., Piubelli, C., Caldrer, S., Riccetti, S., Sinigaglia, A., and Barzon, L. (2021). Antibody response to the BNT162b2 mRNA COVID-19 vaccine in subjects with prior SARS-CoV-2 infection. Viruses *13*, 422. https://doi.org/10.3390/v13030422.
30. Shenoy, P., Ahmed, S., Paul, A., Cherian, S., Umesh, R., Shenoy, V., Vijayan, A., Babu, S., S, N., and Thambi, A. (2022). Hybrid immunity versus vaccine-induced immunity against SARS-CoV-2 in patients with autoimmune rheumatic diseases. Lancet Rheumatol. *4*, e80–e82. https://doi.org/10.1016/s2665-9913(21)00356-8.
31. Prendecki, M., Clarke, C., Brown, J., Cox, A., Gleeson, S., Guckian, M., Randell, P., Pria, A.D., Lightstone, L., Xu, X.N., et al. (2021). Effect of previous SARS-CoV-2 infection on humoral and T-cell responses to single-dose BNT162b2 vaccine. Lancet *397*, 1178–1181. https://doi.org/10.1016/s0140-6736(21)00502-x.
32. Sasikala, M., Shashidhar, J., Deepika, G., Ravikanth, V., Krishna, V.V., Sadhana, Y., Pragathi, K., and Reddy, D.N. (2021). Immunological memory and neutralizing activity to a single dose of COVID-19 vaccine in previously infected individuals. Int. J. Infect. Dis. *108*, 183–186. https://doi.org/10.1016/j.ijid.2021.05.034.
33. Wang, Z., Schmidt, F., Weisblum, Y., Muecksch, F., Barnes, C.O., Finkin, S., Schaefer-Babajew, D., Cipolla, M., Gaebler, C., Lieberman, J.A., et al. (2021). mRNA vaccine-elicited antibodies to SARS-CoV-2 and circulating variants. Nature *592*, 616–622. https://doi.org/10.1038/s41586-021-03324-6.
34. Barrett, J.R., Belij-Rammerstorfer, S., Dold, C., Ewer, K.J., Folegatti, P.M., Gilbride, C., Halkerston, R., Hill, J., Jenkin, D., Stockdale, L., et al. (2021). Phase 1/2 trial of SARS-CoV-2 vaccine ChAdOx1 nCoV-19 with a booster dose induces multifunctional antibody responses. Nat. Med. *27*, 279–288. https://doi.org/10.1038/s41591-020-01179-4.
35. Fiolet, T., Kherabi, Y., MacDonald, C.J., Ghosn, J., and Peiffer-Smadja, N. (2022). Comparing COVID-19 vaccines for their characteristics, efficacy and effectiveness against SARS-CoV-2 and variants of concern: a

narrative review. Clin. Microbiol. Infect. *28*, 202–221. https://doi.org/10.1016/j.cmi.2021.10.005.

36. Puranik, A., Lenehan, P.J., Silvert, E., Niesen, M.J.M., Corchado-Garcia, J., O'Horo, J.C., Virk, A., Swift, M.D., Halamka, J., Badley, A.D., et al. (2021). Comparison of two highly-effective mRNA vaccines for COVID-19 during periods of Alpha and Delta variant prevalence. Preprint at medRxiv. https://doi.org/10.1101/2021.08.06.21261707.

37. Tang, P., Hasan, M.R., Chemaitelly, H., Yassine, H.M., Benslimane, F.M., Al Khatib, H.A., AlMukdad, S., Coyle, P., Ayoub, H.H., Al Kanaani, Z., et al. (2021). BNT162b2 and mRNA-1273 COVID-19 vaccine effectiveness against the SARS-CoV-2 Delta variant in Qatar. Nat. Med. *27*, 2136–2143. https://doi.org/10.1038/s41591-021-01583-4.

38. Rotshild, V., Hirsh-Raccah, B., Miskin, I., Muszkat, M., and Matok, I. (2021). Comparing the clinical efficacy of COVID-19 vaccines: a systematic review and network meta-analysis. Sci. Rep. *11*, 22777. https://doi.org/10.1038/s41598-021-02321-z.

39. Ioannou, G.N., Locke, E.R., Green, P.K., and Berry, K. (2022). Comparison of Moderna versus Pfizer-BioNTech COVID-19 vaccine outcomes: a target trial emulation study in the U.S. Veterans Affairs healthcare system. EClinicalMedicine *45*, 101326. https://doi.org/10.1016/j.eclinm.2022.101326.

40. Li, C., Guo, Y., Fang, Z., Zhang, H., Zhang, Y., and Chen, K. (2022). Analysis of the protective efficacy of approved COVID-19 vaccines against various Mutants. Front. Immunol. *13*, 804945. https://doi.org/10.3389/fimmu.2022.804945.

41. Agrati, C., Castilletti, C., Goletti, D., Sacchi, A., Bordoni, V., Mariotti, D., Notari, S., Matusali, G., Meschi, S., Petrone, L., et al. (2022). Persistent Spike-specific T cell immunity despite antibody reduction after 3 months from SARS-CoV-2 BNT162b2-mRNA vaccine. Sci. Rep. *12*, 6687. https://doi.org/10.1038/s41598-022-07741-z.

42. Neidleman, J., Luo, X., McGregor, M., Xie, G., Murray, V., Greene, W.C., Lee, S.A., and Roan, N.R. (2021). mRNA vaccine-induced T cells respond identically to SARS-CoV-2 variants of concern but differ in longevity and homing properties depending on prior infection status. Elife *10*, e72619. https://doi.org/10.7554/eLife.72619.

43. Sritipsukho, P., Khawcharoenporn, T., Siribumrungwong, B., Damronglerd, P., Suwantarat, N., Satdhabudha, A., Chaiyakulsil, C., Sinlapamongkolkul, P., Tangsathapornpong, A., Bunjoungmanee, P., et al. (2022). Comparing real-life effectiveness of various COVID-19 vaccine regimens during the delta variant-dominant pandemic: a test-negative case-control study. Emerg. Microbes Infect. *11*, 585–592. https://doi.org/10.1080/22221751.2022.2037398.

44. Cerqueira-Silva, T., Andrews, J.R., Boaventura, V.S., Ranzani, O.T., de Araújo Oliveira, V., Paixão, E.S., Júnior, J.B., Machado, T.M., Hitchings, M.D.T., Dorion, M., et al. (2022). Effectiveness of CoronaVac, ChAdOx1 nCoV-19, BNT162b2, and Ad26.COV2.S among individuals with previous SARS-CoV-2 infection in Brazil: a test-negative, case-control study. Lancet Infect. Dis. *22*, 791–801. https://doi.org/10.1016/s1473-3099(22)00140-2.

45. Feng, S., Phillips, D.J., White, T., Sayal, H., Aley, P.K., Bibi, S., Dold, C., Fuskova, M., Gilbert, S.C., Hirsch, I., et al. (2021). Correlates of protection against symptomatic and asymptomatic SARS-CoV-2 infection. Preprint at medRxiv. https://doi.org/10.1101/2021.06.21.21258528.

46. Ramasamy, M.N., Minassian, A.M., Ewer, K.J., Flaxman, A.L., Folegatti, P.M., Owens, D.R., Voysey, M., Aley, P.K., Angus, B., Babbage, G., et al. (2021). Safety and immunogenicity of ChAdOx1 nCoV-19 vaccine administered in a prime-boost regimen in young and old adults (COV002): a single-blind, randomised, controlled, phase 2/3 trial. Lancet *396*, 1979–1993. https://doi.org/10.1016/s0140-6736(20)32466-1.

47. Stephenson, K.E., Le Gars, M., Sadoff, J., de Groot, A.M., Heerwegh, D., Truyers, C., Atyeo, C., Loos, C., Chandrashekar, A., McMahan, K., et al. (2021). Immunogenicity of the Ad26.COV2.S vaccine for COVID-19. JAMA *325*, 1535–1544. https://doi.org/10.1001/jama.2021.3645.

48. Gilbert, P.B., Montefiori, D.C., McDermott, A., Fong, Y., Benkeser, D., Deng, W., Zhou, H., Houchens, C.R., Martins, K., Jayashankar, L., et al. (2021). Immune correlates analysis of the mRNA-1273 COVID-19 vaccine efficacy trial. Preprint at medRxiv. https://doi.org/10.1101/2021.08.09.21261290.

49. Levin, E.G., Lustig, Y., Cohen, C., Fluss, R., Indenbaum, V., Amit, S., Doolman, R., Asraf, K., Mendelson, E., Ziv, A., et al. (2021). Waning immune humoral response to BNT162b2 Covid-19 vaccine over 6 months. N. Engl. J. Med. *385*, e84. https://doi.org/10.1056/NEJMoa2114583.

50. Naaber, P., Tserel, L., Kangro, K., Sepp, E., Jürjenson, V., Adamson, A., Haljasmägi, L., Rumm, A.P., Maruste, R., Kärner, J., et al. (2021). Dynamics of antibody response to BNT162b2 vaccine after six months: a longitudinal prospective study. Lancet Reg. Health. Eur. *10*, 100208. https://doi.org/10.1016/j.lanepe.2021.100208.

51. Gaebler, C., Wang, Z., Lorenzi, J.C.C., Muecksch, F., Finkin, S., Tokuyama, M., Cho, A., Jankovic, M., Schaefer-Babajew, D., Oliveira, T.Y., et al. (2021). Evolution of antibody immunity to SARS-CoV-2. Nature *591*, 639–644. https://doi.org/10.1038/s41586-021-03207-w.

52. Widge, A.T., Rouphael, N.G., Jackson, L.A., Anderson, E.J., Roberts, P.C., Makhene, M., Chappell, J.D., Denison, M.R., Stevens, L.J., Pruijssers, A.J., et al. (2021). Durability of responses after SARS-CoV-2 mRNA-1273 vaccination. N. Engl. J. Med. *384*, 80–82. https://doi.org/10.1056/NEJMc2032195.

53. Goldblatt, D., Fiore-Gartland, A., Johnson, M., Hunt, A., Bengt, C., Zavadska, D., Snipe, H.D., Brown, J.S., Workman, L., Zar, H.J., et al. (2022). Towards a population-based threshold of protection for COVID-19 vaccines. Vaccine *40*, 306–315. https://doi.org/10.1016/j.vaccine.2021.12.006.

54. Garcia-Beltran, W.F., Lam, E.C., St Denis, K., Nitido, A.D., Garcia, Z.H., Hauser, B.M., Feldman, J., Pavlovic, M.N., Gregory, D.J., Poznansky, M.C., et al. (2021). Multiple SARS-CoV-2 variants escape neutralization by vaccine-induced humoral immunity. Cell *184*, 2372–2383.e9. https://doi.org/10.1016/j.cell.2021.03.013.

55. Dejnirattisai, W., Huo, J., Zhou, D., Zahradník, J., Supasa, P., Liu, C., Duyvesteyn, H.M.E., Ginn, H.M., Mentzer, A.J., Tuekprakhon, A., et al. (2022). SARS-CoV-2 Omicron-B.1.1.529 leads to widespread escape from neutralizing antibody responses. Cell *185*, 467–484.e15. https://doi.org/10.1016/j.cell.2021.12.046.

56. Supasa, P., Zhou, D., Dejnirattisai, W., Liu, C., Mentzer, A.J., Ginn, H.M., Zhao, Y., Duyvesteyn, H.M.E., Nutalai, R., Tuekprakhon, A., et al. (2021). Reduced neutralization of SARS-CoV-2 B.1.1.7 variant by convalescent and vaccine sera. Cell *184*, 2201–2211.e7. https://doi.org/10.1016/j.cell.2021.02.033.

57. Bartsch, Y., Tong, X., Kang, J., José Avendaño, M., Serrano, E.F., García-Salum, T., Pardo-Roa, C., Riquelme, A., Medina, R.A., and Alter, G. (2021). Preserved Omicron Spike specific antibody binding and Fc-recognition across COVID-19 vaccine platforms. Preprint at medRxiv. https://doi.org/10.1101/2021.12.24.21268378.

58. Kaplonek, P., Fischinger, S., Cizmeci, D., Bartsch, Y.C., Kang, J., Burke, J.S., Shin, S.A., Dayal, D., Martin, P., Mann, C., et al. (2022). mRNA-1273 vaccine-induced antibodies maintain Fc effector functions across SARS-CoV-2 variants of concern. Immunity *55*, 355–365.e4. https://doi.org/10.1016/j.immuni.2022.01.001.

59. Richardson, S.I., Manamela, N.P., Motsoeneng, B.M., Kaldine, H., Ayres, F., Makhado, Z., Mennen, M., Skelem, S., Williams, N., Sullivan, N.J., et al. (2022). SARS-CoV-2 Beta and Delta variants trigger Fc effector function with increased cross-reactivity. Cell Rep. Med. *3*, 100510. https://doi.org/10.1016/j.xcrm.2022.100510.

60. Herman, J.D., Wang, C., Loos, C., Yoon, H., Rivera, J., Eugenia Dieterle, M., Haslwanter, D., Jangra, R.K., Bortz, R.H., 3rd, Bar, K.J., et al. (2021). Functional convalescent plasma antibodies and pre-infusion titers shape the early severe COVID-19 immune response. Nat. Commun. *12*, 6853. https://doi.org/10.1038/s41467-021-27201-y.

61. Hassan, A.O., Kafai, N.M., Dmitriev, I.P., Fox, J.M., Smith, B.K., Harvey, I.B., Chen, R.E., Winkler, E.S., Wessel, A.W., Case, J.B., et al. (2020). A

single-dose intranasal Chad vaccine protects upper and lower respiratory tracts against SARS-CoV-2. Cell *183*, 169–184.e13. https://doi.org/10.1016/j.cell.2020.08.026.

62. Pardi, N., Tuyishime, S., Muramatsu, H., Kariko, K., Mui, B.L., Tam, Y.K., Madden, T.D., Hope, M.J., and Weissman, D. (2015). Expression kinetics of nucleoside-modified mRNA delivered in lipid nanoparticles to mice by various routes. J. Control. Release *217*, 345–351. https://doi.org/10.1016/j.jconrel.2015.08.007.
63. Cho, A., Muecksch, F., Schaefer-Babajew, D., Wang, Z., Finkin, S., Gaebler, C., Ramos, V., Cipolla, M., Mendoza, P., Agudelo, M., et al. (2021). Anti-SARS-CoV-2 receptor-binding domain antibody evolution after mRNA vaccination. Nature *600*, 517–522. https://doi.org/10.1038/s41586-021-04060-7.
64. Arunachalam, P.S., Walls, A.C., Golden, N., Atyeo, C., Fischinger, S., Li, C., Aye, P., Navarro, M.J., Lai, L., Edara, V.V., et al. (2021). Adjuvanting a subunit COVID-19 vaccine to induce protective immunity. Nature *594*, 253–258. https://doi.org/10.1038/s41586-021-03530-2.
65. Madu, I.G., Roth, S.L., Belouzard, S., and Whittaker, G.R. (2009). Characterization of a highly conserved domain within the severe acute respiratory syndrome coronavirus spike protein S2 domain with characteristics of a viral fusion peptide. J. Virol. *83*, 7411–7421. https://doi.org/10.1128/JVI.00079-09.
66. Ng, K.T., Mohd-Ismail, N.K., and Tan, Y.J. (2021). Spike S2 subunit: the dark horse in the race for prophylactic and therapeutic interventions against SARS-CoV-2. Vaccines *9*, 178. https://doi.org/10.3390/vaccines9020178.
67. Shah, P., Canziani, G.A., Carter, E.P., and Chaiken, I. (2021). The case for S2: the potential benefits of the S2 subunit of the SARS-CoV-2 spike protein as an immunogen in fighting the COVID-19 pandemic. Front. Immunol. *12*, 637651. https://doi.org/10.3389/fimmu.2021.637651.
68. Kaplonek, P., Wang, C., Bartsch, Y., Fischinger, S., Gorman, M.J., Bowman, K., Kang, J., Dayal, D., Martin, P., Nowak, R.P., et al. (2021). Early cross-coronavirus reactive signatures of humoral immunity against COVID-19. Sci. Immunol. *6*, eabj2901. https://doi.org/10.1126/sciimmunol.abj2901.
69. Ng, K.W., Faulkner, N., Cornish, G.H., Rosa, A., Harvey, R., Hussain, S., Ulferts, R., Earl, C., Wrobel, A.G., Benton, D.J., et al. (2020). Preexisting and de novo humoral immunity to SARS-CoV-2 in humans. Science *370*, 1339–1343. https://doi.org/10.1126/science.abe1107.
70. Zimmermann, P., and Curtis, N. (2022). Why does the severity of COVID-19 differ with age?: understanding the mechanisms underlying the age gradient in outcome following SARS-CoV-2 infection. Pediatr. Infect. Dis. J. *41*, e36–e45. https://doi.org/10.1097/inf.0000000000003413.
71. Graham, C., Seow, J., Huettner, I., Khan, H., Kouphou, N., Acors, S., Winstone, H., Pickering, S., Galao, R.P., Dupont, L., et al. (2021). Neutralization potency of monoclonal antibodies recognizing dominant and subdominant epitopes on SARS-CoV-2 Spike is impacted by the B.1.1.7 variant. Immunity *54*, 1276–1289.e6. https://doi.org/10.1016/j.immuni.2021.03.023.
72. Brown, E.P., Licht, A.F., Dugast, A.S., Choi, I., Bailey-Kellogg, C., Alter, G., and Ackerman, M.E. (2012). High-throughput, multiplexed IgG subclassing of antigen-specific antibodies from clinical samples. J. Immunol. Methods *386*, 117–123. https://doi.org/10.1016/j.jim.2012.09.007.
73. Brown, E.P., Dowell, K.G., Boesch, A.W., Normandin, E., Mahan, A.E., Chu, T., Barouch, D.H., Bailey-Kellogg, C., Alter, G., and Ackerman, M.E. (2017). Multiplexed Fc array for evaluation of antigen-specific antibody effector profiles. J. Immunol. Methods *443*, 33–44. https://doi.org/10.1016/j.jim.2017.01.010.
74. Nimmerjahn, F., and Ravetch, J.V. (2008). Fcgamma receptors as regulators of immune responses. Nat. Rev. Immunol. *8*, 34–47. https://doi.org/10.1038/nri2206.
75. Butler, A.L., Fallon, J.K., and Alter, G. (2019). A sample-sparing multiplexed ADCP assay. Front. Immunol. *10*, 1851. https://doi.org/10.3389/fimmu.2019.01851.
76. Karsten, C.B., Mehta, N., Shin, S.A., Diefenbach, T.J., Slein, M.D., Karpinski, W., Irvine, E.B., Broge, T., Suscovich, T.J., and Alter, G. (2019). A versatile high-throughput assay to characterize antibody-mediated neutrophil phagocytosis. J. Immunol. Methods *471*, 46–56. https://doi.org/10.1016/j.jim.2019.05.006.
77. Fischinger, S., Fallon, J.K., Michell, A.R., Broge, T., Suscovich, T.J., Streeck, H., and Alter, G. (2019). A high-throughput, bead-based, antigen-specific assay to assess the ability of antibodies to induce complement activation. J. Immunol. Methods *473*, 112630. https://doi.org/10.1016/j.jim.2019.07.002.

STAR★METHODS

KEY RESOURCES TABLE

REAGENT or RESOURCE	SOURCE	IDENTIFIER
Antibodies		
Pacific Blue™ Mouse Anti-Human CD3	BD Biosciences	CAT#558117 RRID:AB_1595437
Mouse Anti-Human IgG1-Fc PE	Southern Biotech	CAT# 9054-09 RRID:AB_2796628
Mouse Anti-Human IgG2-Fc PE	Southern Biotech	CAT# 9060-09; RRID:AB_2796635
Mouse Anti-Human IgG3-Fc PE	Southern Biotech	CAT# 9210-09; RRID:AB_2796701
Mouse Anti-Human IgM-Fc PE	Southern Biotech	CAT# 9020-09 RRID:AB_2796577
Mouse Anti-Human IgA1-Fc PE	Southern Biotech	CAT# 9130-09 RRID:AB_2796656
Pacific Blue(TM) anti-human CD66b antibody	Biolegend	CAT# 305112 RRID:AB_2563294
Anti-CD107a– phycoerythrin (PE) – Cy5, clone: H4A3	BD	CAT# 555802
Anti-CD56 PE-Cy7 clone: B159	BD	CAT# 560916
Anti-CD16 APC-Cy5, clone: 3G8	BD	CAT# 555408
Anti- CD3 PacBlue, UCHT1	BD	CAT# 558117
MIP1β, clone: D21–1351	BD	CAT# 550078
IFNγ, clone: B27	BD	CAT# 554700
Goat anti-IgG fraction to guinea pig Complement C3-FITC	Mpbio	0855385
Chemicals, peptides, and recombinant proteins		
SARS-CoV-2 Spike protein (S)	Sino Biological	CAT#:40590-V05B
SARS-CoV-2 receptor binding domain (RBD)	Sino Biological	CAT#: 40592-V08H
SARS-CoV-2 N-terminal domain (NTD)	Sino Biological	CAT#:40591-V49H
SARS-CoV-2 subunit 1 of the spike protein (S1)	Sino Biological	CAT#: 40591-V08B1
SARS-CoV-2 subunit 2 of the spike protein (S2)	Sino Biological	CAT#:40590-V08B
SARS-CoV-2 Beta (B.1.351) Spike	Sino Biological	CAT#:40589-V08H13
SARS-CoV-2 Beta (B.1.351) RBD	Sino Biological	CAT#:40592-V08H85-B
SARS-CoV-2 Delta (B.1.617.2) Spike	Sino Biological	CAT#:40589-V08H10
SARS-CoV-2 Delta (B.1.617.2) RBD	Sino Biological	CAT#:40592-V08H90
SARS-CoV-2 Omicron (B.1.1529) Spike	Sino Biological	CAT#:40589-V49H3-B
SARS-CoV-2 Omicron (B.1.1529) RBD	Sino Biological	CAT#:40592-V08H121
SARS-CoV-2 Omicron BA.5 Spike	Sino Biological	CAT#: 40589-V08H32
SARS-CoV-2 Omicron BA.5 RBD	Sino Biological	CAT#: 40592-V08H130
HA A/Michigan/45/2015 (H1N1)	Immune Tech	IT-003-00105DTMp
HA A/Singapore/INFIMH-16-0019/2016 (H3N2)	Immune Tech	IT-003-00434DTMp
HA B/Phuket/3073/2013	Immune Tech	IT-003-B11DTMp
Human Fc receptors	Produced at the Duke Human Vaccine Institute	N/A
Streptavidin-R-Phycoerythrin	Prozyme	CAT#:PJ31S
FIX&Perm Cell Permeabilization Kit	Life Tech	CAT#: GAS001S100 CAT#: GAS002S100

(*Continued on next page*)

Continued

REAGENT or RESOURCE	SOURCE	IDENTIFIER
Brefeldin A	Sigma Aldrich	CAT #: B7651
GolgiStop	BD Biosciences	CAT #: 554724
EDC (1-ethyl-3-(3-dimethylaminopropyl) carbodiimide hydrochloride)	Thermo Fisher	CAT# 77149
Sulfo-NHS-LC-LC biotin	Thermo Fisher	CAT# A35358
Experimental Models: Cell lines		
THP-1 cells	ATCC	CAT# TIB-202
Software and algorithms		
IntelliCyt ForeCyt (v8.1)	Sartorius	https://intellicyt.com/products/software/
FlowJo (v10.7.1)	FlowJo, LLC	https://www.flowjo.com/solutions/flowjo
Prism 9.2.0 (283)	GraphPad	https://www.graphpad.com/scientific-software/prism/
Other		
Yellow-green (505/515) fluorescent Neutravidin-conjugated beads	Thermo Fisher	CAT# F8803
Red-orange(565/580) fluorescent Neutravidin-conjugated beads	Thermo Fisher	CAT# F8794
MagPlex microspheres	Luminex corporation	NA
RosetteSep	STEMCELL	CA# 19665
Lyophilized guinea pig complement	Cedarlane	CA# CL5000-1-R

RESOURCE AVAILABILITY

Lead contact

Further information and requests for resources and reagents should be directed to and will be fulfilled by the lead contact Galit Alter (galter@mgh.harvard.edu).

Materials availability

This study did not generate new unique reagents.

Data and code availability

All anonymized data reported in this paper will be shared by the lead contact upon request. The request should be directed to galter@mgh.harvard.edu. This paper does not report original code. Any additional information required to reanalyze the data reported in this paper is available from the lead contact upon request.

EXPERIMENTAL MODEL AND SUBJECT DETAILS

Description of the cohorts

Samples were collected post-vaccination from groups of individuals receiving the vaccine as part of their government's national rollout campaigns with the verbal consent of participants.[53] The demographic characteristic of the four groups of vaccinees is provided in Table S1. Samples from Latvia and South Africa vaccinees were obtained as part of a previous study of HCWs in pediatric facilities originally initiated at Great Ormond Street Hospital (COSTARS, IRAS 282713, ClinicalTrials.gov Identifier: NCT04380896). Ethics approval was obtained locally by the lead investigators of each site. In the UK, volunteers who were part of the COSTARS Study, as well as others who had received vaccines as part of the government rollout altruistically, agreed to donate serum to help evaluate an assay for measuring post-vaccine immunity being run the UCL laboratory. Vaccinees received one of four vaccines depending on local availability. In Latvia and South Africa, serum was aliquoted, given a unique identifier, and stored frozen until batch shipping to the WHO International Reference laboratory for Pneumococcal Serology at University College London, London, UK. Local UK samples had serum extracted and were stored frozen until batch tested.

Primary immune cells

Fresh peripheral blood was collected by the MGH Blood bank from healthy human volunteers. All volunteers were over 18 years of age, provided written informed consent and all samples were de-identified before use. Information on donor demographics was not

collected. The studies were approved by the MGH (previously Partners Healthcare) Institutional Review Board. Information on donor demographics were not collected. Human NK cells were isolated from fresh peripheral blood and maintained at 37°C, 5% CO_2 in RPMI with 10% fetal bovine serum, L-glutamine, penicillin/streptomycin.

Cell lines

THP-1 cells (ATCC) were grown in RPMI-1640 supplemented with 10% fetal bovine serum, L-glutamine, penicillin/streptomycin, HEPES, and beta-mercaptoethanol at 37°C, 5% CO2.

METHOD DETAILS

Luminex profiling

Antibody isotyping and Fcγ-receptor (FcγR) binding were conducted by multiplexed Luminex assay, as previously described.[72,73] Briefly, SARS-CoV-2 D614G WT Spike-, S1-domain, S2-domain, Receptor Binding Domain (RBD), and N-terminal domain (NTD), as well as Beta (B.1.351) and Delta (B.1.617.2) and Omicron (B.1.1529) and Omicron BA.5 Spike and RBD (purchased from SinoBiological, USA) were used to profile specific humoral immune responses. Antigens were coupled to magnetic Luminex beads (Luminex Corp) by carbodiimide-NHS ester-coupling (Thermo Fisher). Antigen-coupled microspheres were washed and incubated with plasma samples at an appropriate sample dilution (1:500 for IgG1 and all low affinity Fcγ-receptors, and 1:100 for all other readouts) for 2 h at 37°C in 384-well plates (Greiner Bio-One). The high affinity FcR was not tested due to its minimal role in tuning antibody effector function.[74] Unbound antibodies were washed away, and antigen-bound antibodies were detected by using a PE-coupled detection antibody for each subclass and isotype (IgG1, IgG3, IgA1, and IgM; Southern Biotech), and Fcγ-receptors were fluorescently labeled with PE before addition to immune complexes (FcγR2a, FcγR3a; Duke Protein Production facility). After one hour of incubation, plates were washed, and flow cytometry was performed with an IQue (Intellicyt), and analysis was performed on IntelliCyt ForeCyt (v8.1). PE median fluorescent intensity (MFI) is reported as a readout for antigen-specific antibody titers.

Effector functional assays

Antibody-dependent cellular phagocytosis (ADCP), antibody-dependent neutrophil phagocytosis (ADNP), antibody-dependent complement deposition (ADCD), and antibody-dependent NK activation assays were performed as previously described.[75–77] SARS-CoV-2 Spike proteins were coupled to yellow-green (505/515) or red-orange (565/580) fluorescent Neutravidin-conjugated beads (Thermo Fisher) for ADCP/ADNP and ADCD, respectively. Immune complexes were formed by incubating the diluted pooled samples (ADCP and ADNP 1:100 dilution) with the antigen-coupled beads for two h at 37°C. For ADCP, 1.25×10^5 THP-1 cells/mL were added to the immune complexes and incubated for approximately 18 h at 37°C. After the incubation, THP-1 cells were washed and fixed with 4% paraformaldehyde (PFA) (Alfa Aesar). For ADNP, the immune complexes were incubated with 5×10^5 cells/mL of RBC-lysed whole blood for one h at 37°C. After incubation, cells were washed and stained for CD66b+ (Biolegend) to identify neutrophiles and then fixed in 4% PFA. Flow cytometry was performed to identify the percentage of cells that had phagocytosed beads as well as the number of beads that had been phagocytosis (phagocytosis score = % positive cells × Median Fluorescent Intensity of positive cells/10000). The Flow cytometry was performed with 5 Laser LSR Fortessa Flow Cytometer, and analysis was performed using FlowJo V10.7.1.

For ADCD, the antigen-coupled beads were incubated with the diluted pooled samples (1:10 dilution) for two h at 37°C to form immune complexes. The immune complexes were washed, and lyophilized guinea pig complement (Cedarlane) in gelatin veronal buffer with calcium and magnesium (GBV++) (Boston BioProducts) was added for 30 min (complement was reconstituted according to manufacturer's instruction). The deposition of complement was detected by fluorescein-conjugated goat IgG fraction to guinea pig Complement C3 (Mpbio).

All the assays were acquired by flow cytometry with iQue (Intelluicyt), and the analysis was performed using IntelliCyt ForeCyt. The phagocytosis score was calculated (% cells positive × Median Fluorescent Intensity of positive cells) for ADCP and ADNP. ADCD was reported as the median of C3 deposition.

For antibody-dependent NK cell degranulation, SARS-CoV-2 antigens were coated to 96-well ELISA at the protein concentration of 2 μg/mL, incubated at 37°C for 2hrs and blocked with 5% BSA at 4°C overnight. NK cells were isolated from whole blood from healthy donors (by negative selection using RosetteSep (STEMCELL) then separated using a ficoll gradient. NK cells were rested overnight in media supplemented with IL-15. Serum samples were diluted at 1:25. After blocking, samples were added to coated plates, and immune complexes were formed for two hours at 37°C. After the two hours, NK cells were prepared (antiCD107a– phycoerythrin (PE) – Cy5 (BD, 1:40, clone: H4A3), brefeldin A (10 μg/mL) (Sigma), and GolgiStop (BD)), and added to each well. for 5 h at 37°C. The cells were stained for surface markers using anti-CD56 PE-Cy7 (BD, 1:200, clone: B159), anti-CD16 APC-Cy5 (BD, 1:200, clone: 3G8), and anti- CD3 PacBlue (BD, 1:800, UCHT1) and permeabilized with FIX & PERM Cell Permeabilization Kit (Thermo Fisher). After permeabilization, cells were stained for intracellular markers MIP1β (BD, 1:50, clone: D21–1351) and IFNγ (BD, 1:17, clone: B27). The flow cytometry was performed. NK cells were defined as $CD3^{-}CD16^{+}CD56^{+}$ and frequencies of degranulated (CD107a+), INFγ+ and MIP1β+ NK cells determined on an iQue analyzer (Intellicyt).

QUANTIFICATION AND STATISTICAL ANALYSIS

Univariate comparison

Data analysis was performed using R version 4.1.2. Univariate comparisons between four different vaccine platforms were performed using the Wilcoxon-signed rank test followed by Benjamini-Hochberg (BH) correction. The visualization was performed by the function ''ggplot'' of R package ''ggplot2'' (3.3.5), and the *P-value* was estimated by the function ''wilcox.test'' and ''p.adjust'' in the R package ''stats''(4.1.2) and labeled by the function ''stat_pvalue_manual'' in the R package ''ggpubr'' (0.4.0). The heatmap showing the difference between median of hybrid immunity group vs. that of vaccination only group in log10 scale was plotted by ''heatmap'' function of python module ''seaborn'' (0.11.2), the *P* value was estimated by the function ''mannwhitneyu'' of python module ''scipy.stats'' (1.8.0), followed by the Benjamini-Hochberg procedure of multiple testing correction using function ''multipletests'' of python module ''statsmodels.stats.multitest'' (0.13.2).

Multivariate classification

Classification models were trained to discriminate between vaccination only and hybrid immunity individuals using all the measured antibody responses. Prior to analysis, all data were normalized using z-scoring. Models were built using a combination of the least absolute shrinkage and selection operator (LASSO) for feature selection and then classification using partial least square discriminant analysis (PLS-DA) with the LASSO-selected features (54) using R package ''ropls'' version 1.26.4 (Thévenot et al., 2015) and ''glmnet'' (4.1.3). Model accuracy was assessed using five-fold cross-validation. For each test fold, LASSO-based feature selection was performed on logistic regression using the training set for that fold. LASSO was repeated 10 times, features selected at least 7 times out of 10 were identified as selected features. PLS-DA classifier was applied to the training set using the selected features, and prediction accuracy was recorded. The first two latent variables (LVs) of the PLS-DA model were used to visualize the samples.

Correlation analysis

Spearman correlations were used to correlation between antibody titers and functional responses and were performed using function ''spearmanr'' of python module ''scipy.stats'' (1.8.0). The significance of correlation was adjusted by the Benjamini-Hochberg procedure of multiple testing correction using function ''multipletests'' of python module ''statsmodels.stats.multitest'' (0.13.2).

Defining signatures of previous infection while also controlling for potential cofounders

We accessed the significance of the association between measured antibody levels and the previous infection state by controlling for collected potential cofounders using two nested mixed linear models (null and full model) without/with demographical data, i.e., age and gender in this study. We fit two linear mixed models and estimated the improvement in model fit by likelihood ratio testing to assess how many measurements have a significantly better fit with the full model at a threshold of <0.05.

Null model

$$\text{antibody.measurement} \sim \text{age} + \text{gender} + \text{random.effect}$$

Full model

$$\text{antibody.measurement} \sim \text{age} + \text{gender} + \text{previous.infected} + \text{random.effect}$$

Likelihood ratio test LRT=-2*ln(MLE in Full model MLT in Null model)$\sim\lambda 2$, MLE denotes maximum likelihood estimation and MLT denotes maximum likelihood ratio.

Here, we consider the measurement of IgG1 titer in HA_control as the random effect. The R package ''lme4'' was used to fit the linear mixed model to each measurement and test for measurement across the contrast of interest. The *P* value from the likelihood ratio test and *t* value of previous infected state in full model were visualized as volcano plot using the ''ggplot'' function in R package ''ggplot2''.